Final Report

to the

CENTER FOR MULTIMODAL SOLUTIONS FOR CONGESTION MITIGATION (CMS)

CMS Project Number: 2009-012

Title: Robust Congestion Pricing under Boundedly Rational Travel Behaviors

for period 5/15/2009 to 12/31/2010

from Yingyan Lou, Yafeng Yin* and Siriphong Lawphongpanich
*Department of Civil and Coastal Engineering
University of Florida
Email: yafeng@ce.ufl.edu (Yafeng Yin)

Date prepared 12/31/2010

DISCLAIMER AND ACKNOWLEDGMENT

The contents of this report reflect the views of the authors, who are responsible for the facts and the accuracy of the information presented herein. This document is disseminated under the sponsorship of the Department of Transportation University Transportation Centers Program, in the interest of information exchange. The U.S. Government assumes no liability for the contents or use thereof.

This work was sponsored by a grant from the Center for Multimodal Solutions for Congestion Mitigation, a U.S. DOT Tier-1 grant-funded University Transportation Center. The authors wish to thank Hongli Xu and Jing Zhou at Nanjing University, China for their collaboration on the development of the prospect-based user equilibrium model.

TABLE OF CONTENTS

DISCLAIMER AND ACKNOWLEDGMENT i

LIST OF TABLES iii

LIST OF FIGURES iv

ABSTRACT vi

EXECUTIVE SUMMARY vii

CHAPTER 1 BACKGROUND 1

CHAPTER 2 PRICING DETERMINISTIC NETWORKS 3

- Introduction 3
- Boundedly Rational User Equilibrium 4
- Congestion Pricing with Boundedly Rational User Equilibrium 14

CHAPTER 3 PRICING STOCHASTIC NETWORKS 25

- Introduction 25
- Basic Considerations 26
- Prospect-Based User Equilibrium 31
- Solution Algorithm and Numerical Examples 34
- Behaviorally Consistent Congestion Pricing 44

CHAPTER 4 CONCLUDING REMARKS 50

REFERENCE 51

LIST OF TABLES

Table		Page
2-1	Flow Distributions for the Bridge Network	8
2-2	Flow Distributions for the Bridge Network	10
2-3	Flow Distributions for the Nine-Node Network ($\alpha = 0.10$)	12
2-4	Pricing Schemes and Their Performances for the Nine-Node Network	21
3-1	Traveler Characteristics	36
3-2	Prospect-Based User Equilibrium Path Flow Pattern	37
3-3	Comparisons of Link Flow Patterns from Three Different UE Models	37
3-4	Link Characteristics of the Example Network	39
3-5	Traveler Characteristics	39
3-6	Prospect-Based User Equilibrium Path Flow Pattern for O-D Pair 4-2 ($\sigma = \sigma_1$)	40
3-7	Prospect-Based User Equilibrium Path Flow Pattern for O-D Pair 4-3 ($\sigma = \sigma_1$)	41
3-8	Prospect-based user equilibrium path flow pattern for O-D pair 4-2 ($\sigma = \sigma_2$)	43
3-9	Comparisons of System Performances	44
3-10	Optimum Toll Pattern and the Tolled Prospect-Based User Equilibrium Flow	48
3-11	Tolled Prospect-Based UE Path Flow Pattern for O-D Pair 1-3 ($\sigma = \sigma_1$)	49

LIST OF FIGURES

Figure Page

2-1 A bridge network 7

2-2 Relationship between three different flow sets 9

2-3 The nine-node network 11

2-4 Comparison of system performances of BRUE at the nine-node network 13

2-5 Comparison of system performances of BRUE at the Sioux Falls network 14

2-6 System performances with MC pricing scheme at the nine-node network 15

2-7 Three-parallel-link network 15

2-8 Comparison of worst-case total travel times with no toll, robust and MC tolls at the nine-node network 22

2-9 System performances with MC and RT1 at the nine-node network 23

2-10 System performances with MC and RT1 at the nine-node network 24

3-1 Value function 28

3-2 Weighting function 28

3-3 Four-link network 36

3-4 Nguyen and Dupuis's network 38

3-5 Prospect values of paths between O-D pairs 4-2 and 4-3 40

3-6 Equilibrium reference points and travel prospects between O-D pair 4-2 42

3-7 Equilibrium reference points and travel prospects between O-D pair 4-3 42

3-8 Convergence plot 48

ABSTRACT

Congestion pricing is a market-based approach for mitigating traffic congestion and managing travel demand. For over 80 years, the literature on congestion pricing has been largely relying on the assumption that travelers are perfectly (or unboundedly) rational. Although technically convenient, this assumption implies that travelers are always able to react to pricing signals and accurately select the options with the least cost to reach their destinations. However, there is abundant empirical evidence that travelers are boundedly rational and their responses to pricing signals are not as perfect as assumed in pricing models reported in the literature. Consequently, congestion pricing projects may not achieve the results predicted by these models.

This report proposes methodologies for determining pricing strategies that can better relieve congestion by proactively accounting for travelers with bounded rationality. Two classes of models are addressed. As adopted by many in the literature, one class assumes that link travel times (or costs) are deterministic. In the other class, the travel times are probabilistic and the analysis of the traveler's route choice is based on the cumulative prospect theory, a paradigm for decision making under uncertainty advanced recently by psychologists and behavioral economists. For both classes of models, new optimization problems and algorithms are developed to accommodate boundedly rational travel behaviors to determine more robust or reliable pricing schemes.

EXECUTIVE SUMMARY

The report provides analytical foundations and methodologies for the design and analysis of congestion pricing strategies for transportation networks under a more convincing behavioral assumption, i.e., travelers are boundedly rational.

For more than 80 years, the literature on congestion pricing has been relying largely on the assumption that travelers are perfectly rational. Although technically convenient, this assumption implies that travelers are always able to react to pricing signals and accurately select the options with the least cost to reach their destinations. However, empirical studies reveal that travelers are perfectly rational instead. For example, travelers have a general aversion to complex pricing structures. Increasing complexity makes travelers more likely to remain with the status quo. Moreover, they switch to a cheaper option only when the amount of saving is sufficiently large. This suggests that the current models of congestion pricing are not consistent with the actual traveler behaviors. Such inconsistence may lead to inferior pricing policies that are not able to reduce congestion to the expected extent or even worsen the situation. A new modeling approach is needed to account for this bounded rationality in the design of congestion pricing schemes.

The main objective of this report is two-fold. One is to study the effect or implication of boundedly rational travel behavior on the design and evaluation of congestion pricing strategies, and the other is to develop analytical frameworks to proactively account for this behavior when designing pricing strategies for transportation networks.

The investigation considers both deterministic and stochastic networks. The former assumes that link travel times or costs are deterministic, an assumption adopted by many in the literature. When they are boundedly rational, users do not necessarily choose a shortest or cheapest route when doing so does not reduce their travel times by a significant amount. A general path-based definition and a more restrictive link-based representation of boundedly rational user equilibrium (BRUE) are presented in the report. The set of BRUE flow distributions is non-empty and generally non-convex. The problems of finding best- and worst-case BRUE flow distributions are formulated and solved as mathematical programs with complementarity constraints. Because alternative tolled BRUE flow distributions exist, our congestion pricing models seek a toll vector or pattern that minimizes the system travel time of the worst-case tolled BRUE flow distribution. As formulated, the models are generalized semi-infinite min-max problems and a heuristic algorithm based on penalty functions and cutting-planes is proposed to solve them. Numerical examples are presented to illustrate key concepts and results.

The second part of the report is on pricing stochastic networks where travel times or costs are stochastic, a condition caused by day-to-day demand variations and traffic incidents. Given that the cumulative prospect theory provides a well-supported descriptive paradigm for decision making under risk or uncertainty, previous studies applied the theory to model travelers' route choice behaviors in stochastic networks and developed prospect-based user equilibrium models. The models rely on exogenous inputs of reference points and thus the resulting reference-dependence could be regarded as an ad-hoc assumption. This report proposes a premise regarding travelers' determination of reference points and encapsulates it into the prospect-based user equilibrium conditions. The conditions are formulated as an equivalent variational inequality, and a heuristic solution algorithm is proposed to solve it. Both the model and the solution algorithm are demonstrated with two numerical examples. This report further develops an optimal pricing model in which the proposed user equilibrium model is adopted to capture travelers' response to pricing signals under risk. The pricing model is formulated as a mathematical program with complementarity constraints, solved by a derivative-free algorithm. Another numerical example is presented to illustrate the pricing model and the solution algorithm.

The behaviorally consistent pricing framework proposed in this report is novel and distinct from others in the congestion pricing literature. As congestion increases in the coming years, we envision a widespread adoption of congestion pricing in some form across the country. The proposed pricing framework will help to ensure successful implementations and save substantial amount of time and money that the traveling public have to spend waiting in traffic congestion.

1. BACKGROUND

Congestion pricing has been advocated as an efficient way for congestion mitigation since the seminal work by Pigou (1920) and Knight (1924) (see Lindsey, 2006, for a recent review). The basic idea is to charge tolls to influence travelers' choices of travel to reduce traffic congestion and improve social welfare. Examples from abroad include the cordon or area-based pricing in Singapore, London and Stockholm among others. In the U.S., a more prevalent form of congestion pricing is variably priced lanes, such as high-occupancy/toll (HOT) lanes where high-occupancy vehicles can travel for free while lower-occupancy vehicles have to pay a fee to access. In May 2006, the U.S. Department of Transportation (USDOT) launched a new national congestion relief initiative that promotes congestion pricing (USDOT, 2006).

For more than 80 years, the literature on congestion pricing has been largely relying on the assumption that travelers are perfectly (or unboundedly) rational. Although technically convenient, this assumption implies that travelers can always react to pricing signals and select the options with the least cost to reach their destinations. However, empirical studies reveal that travelers are boundedly rational instead. For example, travelers have a general aversion to complex pricing structures and increasing complexity makes them more likely to stay with the status quo. Moreover, they switch to a cheaper option only when the amount of saving is sufficiently large (e.g., Bonsall et al., 2007; Holguin-Veras et al., 2007).

Since its introduction by Nobel Laureate Herbert Simon (Simon, 1955), the notion of bounded rationality has been of interest to psychologists and behavioral economists for more than half a century. There is abundant amount of empirical evidence to support the notion, particularly in the context of day-to-day choices (Conlisk, 1996). Bounded rationality assumes two types of bounds, i.e., the limits on knowledge or information, and the limits on the ability to compute optima. More specifically, perfectly rational decisions often depend on perfect knowledge or information that is unfortunately not always available or too costly to obtain. On the other hand, human cognition is a scarce resource and individuals tend to avoid long deliberation to reach the best decision on many day-to-day choices.

In transportation, the literature on boundedly rational decision is significantly more limited and more recent. Mahmassani and Chang (1987) studied the departure time choice by boundedly rational travelers in an idealized setting that consists of one origin-destination (O-D) pair and a single route. Later, Jayakrishnan et al. (1994), Hu and Mahmassani (1997), Mahmassani and Liu (1997), and Mahmassani (2000) applied the concept and similar models to study, e.g., the effects of provision of advanced traffic information on road systems. Similar to

Conlisk (1996), Nakayama et al. (2001) concluded that their experimental study indicates a need to evaluate the validity of the perfect rationality assumption in the traffic equilibrium analysis.

This report studies the effect or implication of boundedly rational travel behavior on the design and evaluation of congestion pricing strategies, and develops analytical frameworks to account for this behavior more proactively to determine more effective pricing strategies for transportation networks. Although travelers' responses to congestion pricing are multifaceted, this report focuses on their adjustments on route choices over transportation networks. The pricing schemes of interest are static, i.e., time-invariant tolls during peak hours, because (i) empirical studies have shown that implementation of system-wide dynamic pricing is behaviorally infeasible. The pricing signals would be too complex for travelers to understand and predict, not mentioning to react to (e.g., Bonsall et al., 2007); (ii) the derivation of dynamic pricing schemes relies on dynamic traffic assignment, which is computationally intractable for large-scale networks (e.g., Wie, 2007). Moreover, dynamic traffic assignment requires the knowledge of dynamic O-D demand, a type of information generally believed to be difficult to obtain accurately or otherwise.

In the subsequent chapters, we describe our research on both deterministic and stochastic networks. The former implies that link travel times or costs are deterministic, an assumption adopted for almost all pricing models in the literature. In the latter, travel times or costs are stochastic, incurred by day-to-day incidents, such as adverse weather, traffic accidents and disabled cars.

2. PRICING DETERMINISTIC NETWORKS

2.1 INTRODUCTION

This chapter addresses boundedly rational route choice behaviors in deterministic networks where travel times or costs are deterministic and boundedly rational user equilibrium (BRUE) arises whenever all users' travel costs are not sufficiently larger than the best available ones and no user has an incentive to switch his or her route. The focus of this chapter is to study the implication of BRUE in transportation systems planning and develop an analytical framework to proactively account for boundedly rational travel behaviors in the context of congestion pricing. We also note that there are other network equilibrium models in the literature that attempt to describe more realistically users' route choice behaviors, such as stochastic user equilibrium models (e.g., Sheffi, 1985), risk-taking models (e.g., Mirchandani and Sourosh, 1987; Yin and Ieda, 2001), travel time budget models (e.g., Lo et al. 2006; Shao et al., 2006). The purpose of this chapter is to offer another alternative model that enriches the literature and to fully explore the properties and consequences of bounded rationality in route choices. More specifically, as Mahmassani and Chang (1987) point out and discussed below, BRUE flow distributions in a static network may not be unique and we characterize the set of all possible BRUE flow distributions as a non-convex and non-empty set. In one interpretation, the flow distribution we observe at one particular day is just a particular realization from the set. Such an uncertainty incurred by boundedly rational travel behaviors may deteriorate the effectiveness of traditional congestion pricing strategies. For example, the link-based marginal-cost (MC) pricing scheme commonly advocated in the congestion pricing literature may not necessarily reduce congestion to its minimum level because users may not switch to routes with the least generalized cost. In this chapter, we seek a tolling pattern that minimizes the worst-case system travel delay among all the possible BRUE flow patterns based on generalized costs (time plus tolls).

For the remainder, Section 2.2 mathematically defines BRUE and discusses the property of the set of all possible BRUE flow patterns. The problems of finding the best- and worst-case system travel times among the possible BRUE flow patterns are formulated as mathematical programs with complementarity constraints (MPCC) and then illustrated with examples. Section 2.3 formulates congestion pricing models that minimizes the worst-case system travel time and develops a heuristic solution algorithm to the models. Numerical examples are then presented to demonstrate and validate the models and solution algorithm.

2.2 BOUNDEDLY RATIONAL USER EQUILIBRIUM

2.2.1 Boundedly Rational Flow Distribution and Equilibrium Conditions

As explained in Mahmassani and Chang (1987) and Chen et al. (1997), travelers with bounded rationality still follow the behavior that exhibits a tendency toward utility maximization, but not necessarily to the absolute maximum level. We thus define travelers with bounded rationality as those who (a) always choose routes with no cycle and (b) do not necessarily switch to the shortest (cheapest) routes when the difference between the travel times (or costs) on their current routes and the shortest one is no larger than a threshold value.

Using the terminology in Ahuja et al. (1992), all utilized routes under bounded rationality must correspond to paths. In the literature, some prefer to add the adjective “simple” and refer to routes with no cycle as “simple paths.” (Ahuja et al., 1992, refer to routes with cycles as “walks.”) Below are formal definitions of acceptable paths and BRUE:

Definition 2.1: A path is “acceptable” if the difference between its travel time or cost and that of the shortest or least-cost path is no larger than a pre-specified threshold value.

Definition 2.2: A path flow distribution is in BRUE if it is feasible or compatible with the travel demands and every user uses an acceptable path.

Unlike the conventional or perfectly rational user equilibrium (PRUE), the flow distribution under BRUE as defined above may not utilize any shortest or least-cost path. To mathematically define BRUE, let W denote the set of O-D pairs and q^w represent travel demand for O-D pair $w \in W$. Let P^w be the set of paths for O-D pair w. For each path $r \in P^w$, f_r^w and c_r^w denote the corresponding path flow and path travel time. We further use f^w to represent a vector of path flows for O-D pair w, with f_r^w as its elements, and $f = \left(f^1, \cdots f^w, \cdots f^{|W|}\right)^T$, where $|\bullet|$ denotes the cardinality of a set. Similarly, c^w is a vector of path travel times for O-D pair w and c is a vector of c^w. Assuming that users of the same O-D pair have the same threshold value, denoted as $\bar{\varepsilon}^w$, f is a BRUE distribution if and only if there exists λ^w for every w such that:

$$
\begin{aligned}
& c_r^w \geq \lambda^w && \forall\ r \in P^w \\
& c_r^w \leq \lambda^w + \bar{\varepsilon}^w && \forall\ r \in P_+^w = \{r:\ f_r^w > 0, r \in P^w\} \\
& \sum_{r \in P^w} f_r^w = q^w && \\
& f_r^w \geq 0 && \forall\ r \in P^w
\end{aligned}
$$

If f is a BRUE distribution, then setting $\lambda^w = \bar{c}^w$, where $\bar{c}^w$ is the shortest path length for O-D pair w, satisfies the above conditions. On the other hand, if f is a flow distribution with λ^w satisfying the above conditions, then $c_r^w \leq \lambda^w + \bar{\varepsilon}^w \leq \min_{r \in P^w}\{c_r^w\} + \bar{\varepsilon}^w = \bar{c}^w + \bar{\varepsilon}^w$ for every utilized path r. The latter implies that λ^w need not be the length of the shortest path. In general, λ^w is a lower bound for $\bar{c}^w$.

The above conditions requiring knowing utilized paths. As an alternative, the ones below use slack variables ε_r^w and do not require the utilized-path information.

$$c_r^w - \lambda^w - \varepsilon_r^w = 0 \qquad \forall r \in P^w, w \in W \qquad (2.1)$$

$$f_r^w(\bar{\varepsilon}^w - \varepsilon_r^w) \geq 0 \qquad \forall r \in P^w, w \in W \qquad (2.2)$$

$$\sum_{r \in P^w} f_r^w = q^w \qquad \forall w \in W \qquad (2.3)$$

$$f_r^w \geq 0 \qquad \forall r \in P^w, w \in W \qquad (2.4)$$

$$\varepsilon_r^w \geq 0 \qquad \forall r \in P^w, w \in W \qquad (2.5)$$

Note that when $\bar{\varepsilon}^w = 0$ for all *w*, the BRUE conditions reduce to the conventional PRUE conditions. To illustrate, combining (2.2), (2.4) and (2.5) yields $f_r^w \varepsilon_r^w = 0$. Together with (2.1), this implies that $f_r^w(c_r^w - \lambda^w) = 0$, $\forall r \in P^w, w \in W$. On the other hand, a PRUE flow distribution always satisfies (2.1) - (2.5) with $\varepsilon_r^w = 0$ and λ^w as the equilibrium O-D travel time. Thus, a PRUE distribution is always a BRUE flow distribution.

2.2.2 Properties of BRUE Flow Distributions

When users are perfectly rational, it is well-known (see, e.g., Patriksson, 1994) that there exist equivalent link-based equilibrium conditions and the set of all PRUE flow patterns is convex. Below, we show that these properties may not hold when users are boundedly rational. More specifically, the link-based representation of BRUE proposed here is not equivalent to the path-based definition and the set of BRUE flows may not be unique.

2.2.2.1 Link-based Representation of BRUE

Let *N* and *L* denote the sets of nodes and links in a road network, where an element of the latter, *L*, is denoted as (*i*, *j*). For O-D pair *w*, x_{ij}^w represents flow on link (*i*, *j*). The vector x^w denotes the flow vector for O-D pair *w* with x_{ij}^w as its elements, and $v = \sum_w x^w$ is the associated aggregate flow vector. For each link $(i, j) \in L$, $t_{ij}(v_{ij})$ denotes link travel time function that is continuous and monotonically increasing with the aggregate link flow, v_{ij}. Moreover, $t_{ij}(v_{ij}) > 0$ when $v_{ij} > 0$. Let $o(w)$ and $d(w)$ represent the origin and destination of O-D pair *w*, Δ the node-link incidence matrix and *D* the demand vector satisfying that $D_{o(w)}^w = q^w$ or $D_{d(w)}^w = -q^w$ and $D_i^w = 0$ for all other *i*. The following are link-based BRUE conditions, analogous to those under the perfectly rational assumption:

$$t_{ij}(v_{ij}) + \pi_i^w - \pi_j^w - \varepsilon_{ij}^w = 0 \qquad \forall w \in W,\ (i, j) \in L \qquad (2.6)$$

$$x_{ij}^w\left(-\varepsilon_{ij}^w + \mu_i^w - \mu_j^w\right) \geq 0 \qquad \forall w \in W,\ (i, j) \in L \qquad (2.7)$$

$$-\mu_{d(w)}^w \leq \bar{\varepsilon}^w - \mu_{o(w)}^w \qquad \forall w \in W \qquad (2.8)$$

$$\Delta x^w = D^w \qquad \forall w \in W \qquad (2.9)$$

$$v = \sum_w x^w \qquad (2.10)$$

$$x, \varepsilon \geq 0 \qquad (2.11)$$

where $\pi^w \in R^{|N|}$, $\varepsilon^w \in R^{|L|}$ and $\mu^w \in R^{|N|}$ are vectors of node potentials associated with travel time, travel times in excess of the minimum, and node potentials associated with the excess travel times respectively.

When $\bar{\varepsilon}^w = 0$, (2.6) – (2.11), as before, reduce to the linked-based PRUE conditions in the literature when users are perfectly rational. When $\bar{\varepsilon}^w > 0$, we show below that a flow distribution satisfying (2.6) – (2.11) is a BRUE flow (see Definition 2.2). However, as a counterexample below illustrates, the converse is not true.

Lemma 2.1: Define a sub-network G^w with respect to each O-D pair *w*, which consists of all the links with strictly positive O-D flows x_{ij}^w. If there exist a link flow distribution *v*, vectors $\pi^w \in R^{|N|}$, $\varepsilon^w \in R^{|L|}$ and $\mu^w \in R^{|N|}$ satisfying (2.6) – (2.11), then the sub-network G^w is acyclic.

Proof: Suppose that there is a cycle in G^w. By definition, $x_{ij}^w > 0$ for each link $(i, j) \in G^w$. Condition (2.7) then requires $-\varepsilon_{ij}^w + \mu_i^w - \mu_j^w \geq 0$. Thus, summing (2.6) and (2.7) along the cycle leads to

$$\sum_{ij} t_{ij}(v_{ij}) = \sum_{ij} \varepsilon_{ij}^w \leq 0 \qquad (2.12)$$

However, since $v_{ij} \geq x_{ij}^w > 0$, we have $t_{ij}(v_{ij}) > 0$, which contradicts (2.12). Therefore G^w is acyclic. □

Note that Lemma 2.1 also applies to PRUE flow distributions when the travel time functions satisfy our earlier assumptions.

Theorem 2.1: For a link flow distribution *v*, if there exist $\pi^w \in R^{|N|}$, $\varepsilon^w \in R^{|L|}$ and $\mu^w \in R^{|N|}$ such that (2.6) – (2.11) hold, then any of its underlying path flow patterns satisfies the BRUE definition (Definition 2.2).

Proof: Assume that a link flow distribution *v* satisfies (2.6) – (2.11). Then, (2.9) – (2.11) imply that *v* is a feasible flow distribution; and Lemma 2.1 ensures that the flow-carrying sub-networks are acyclic and the underlying utilized routes are all paths. Let δ_{ij}^r (equals 0 or 1) indicates whether link (*i, j*) is on path *r*. It follows from (2.6) and (2.11) that for any path between O-D pair *w*,

$$\pi_{d(w)}^{w} - \pi_{o(w)}^{w} = \sum_{ij} \delta_{ij}^{r} t_{ij}(v_{ij}) - \sum_{ij} \delta_{ij}^{r} \varepsilon_{ij}^{w} \leq \sum_{ij} \delta_{ij}^{r} t_{ij}(v_{ij}) \tag{2.13}$$

Therefore, $\pi_{d(w)}^{w} - \pi_{o(w)}^{w}$ is a lower bound of $\bar{c}^{w}$, the minimum travel time between a given O-D pair *w*. For any utilized path $r \in P_{+}^{w}$ with respect to the given link flow distribution, the flow on each link along the path must be positive, i.e., $x_{ij}^{w} > 0$ if $\delta_{ij}^{r} = 1$. Thus summing together (2.7) for links on a utilized path $r \in P_{+}^{w}$ yields:

$$\sum_{ij} \delta_{ij}^{r} \varepsilon_{ij}^{w} \leq \mu_{o(w)}^{w} - \mu_{d(w)}^{w} \tag{2.14}$$

Essentially $\mu_{o(w)}^{w} - \mu_{d(w)}^{w}$ is an upper bound on the amount in excess of the shortest travel time. Combining (2.8), (2.13) and (2.14) for a utilized path *r* leads to:

$$\sum_{ij} \delta_{ij}^{r} t_{ij}(v_{ij}) - \bar{c}^{w} \leq \sum_{ij} \delta_{ij}^{r} t_{ij}(v_{ij}) - (\pi_{d(w)}^{w} - \pi_{o(w)}^{w}) = \sum_{ij} \delta_{ij}^{r} \varepsilon_{ij}^{w} \leq \mu_{o(w)}^{w} - \mu_{d(w)}^{w} \leq \bar{\varepsilon}^{w}$$

which implies that for any utilized path, its travel time may differ at most the threshold value from the minimum O-D travel time. Therefore, any underlying path pattern of *v* is at BRUE. □

On the other hand, a BRUE flow distribution may not satisfy (2.6) – (2.11). This implies that the link-based representation of BRUE is more restrictive than the path-based definition. Consider the bridge network in Figure 2-1 in which there is only one O-D pair (1, 4) with a demand of 3 and a threshold value of 4. The link travel time functions are reported in Table 2-1 together with a BRUE path flow pattern.

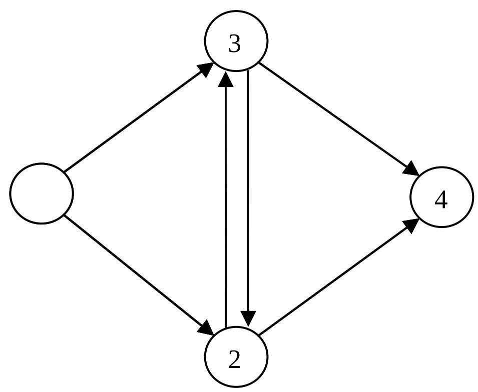

Figure 2-1. A bridge network

Table 2-1. Flow Distributions for the Bridge Network

		BRUE	
		Flow	Time
Link	Travel time function		
(1, 3)	$t_{13} = 3 + v_{13}$	2	5
(1, 2)	$t_{12} = 7 + v_{12}$	1	8
(2, 3)	$t_{23} = v_{23}$	1	1
(2, 4)	$t_{24} = 5 + v_{24}$	1	6
(3, 2)	$t_{32} = v_{32}$	1	1
(3, 4)	$t_{34} = 2 + v_{34}$	2	4
Path			
1-3-4		1	9
1-3-2-4		1	12
1-2-3-4		1	13
1-2-4		0	14

The minimum O-D travel time is 9 and all the utilized paths have travel times of no more than 9 + 4 = 13. Therefore, the path flow pattern is a valid BRUE flow. However, the corresponding link flows do not satisfy (2.6) – (2.11), as the following system of equations does not admit a solution:

$$
\begin{cases}
5-\varepsilon_{13}+\pi_1-\pi_3=0\\
8-\varepsilon_{12}+\pi_1-\pi_2=0\\
1-\varepsilon_{23}+\pi_2-\pi_3=0\\
6-\varepsilon_{24}+\pi_2-\pi_4=0\\
1-\varepsilon_{32}+\pi_3-\pi_2=0\\
4-\varepsilon_{34}+\pi_3-\pi_4=0\\
\varepsilon_{12}+\varepsilon_{24}\le 4\\
\varepsilon_{12}+\varepsilon_{23}+\varepsilon_{34}\le 4\\
\varepsilon_{13}+\varepsilon_{32}+\varepsilon_{24}\le 4\\
\varepsilon_{13}+\varepsilon_{34}\le 4\\
\varepsilon_{ij}\ge 0
\end{cases}
$$

The nonequivalence between the two sets of conditions originates from the relationship between path and link flows. Under BRUE, it is possible that a path flow pattern results in a cyclic flow-carrying sub-network (the original network in the above example) while with the link-based BRUE definition, all the flow-carrying sub-networks must be acyclic (Lemma 2.1). Moreover, for a non-utilized path that only consists of links with positive flows (path 1-2-4 in the above example), the link-based BRUE definition still requires its travel time to be within the indifference band even when the path is not utilized (conditions 2.6 and 2.7). Note that both issues do not arise in the PRUE because 1) the flow-carrying sub-networks are acyclic under PRUE; and 2) all links with positive flows must be on shortest paths. For a non-utilized path that consists of only positive-flow links, its travel time will be minimum O-D travel time and condition (2.6) and (2.7) alike will be satisfied automatically.

Below, Figure 2-2 illustrates the relationship between the feasible flow set, the path-based and the link-based BRUE flow set. Note that all three sets contain the PRUE flow distribution.

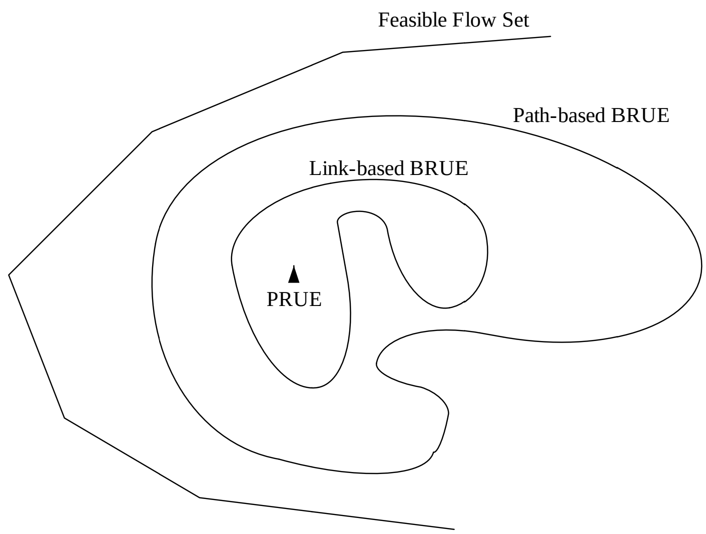

Figure 2-2 Relationship between three different flow sets

2.2.2.2 Nonconvexity

To illustrate that the set of BRUE flows is not convex, consider the same network in Figure 2-1 with one O-D pair (1, 4) as before. However, other problem parameters are new. The travel time functions are as shown in Table 2-2. The demand and a threshold value are 6 and 15, respectively.

Table 2-2. Flow Distributions for the Bridge Network

		BRUE-1		BRUE-2		0.5×(BRUE-1+BRUE-2)	
		Flow	Time	Flow	Time	Flow	Time
Link	Travel time function						
(1, 3)	$t_{13} = 10v_{13}$	3	30	4	40	3.5	35
(1, 2)	$t_{12} = 50 + v_{12}$	3	53	2	52	2.5	52.5
(2, 3)	$t_{23} = v_{23}$	0	0	2	2	1	1
(2, 4)	$t_{24}= 10\ v_{24}$	3	30	4	40	3.5	35
(3, 2)	$t_{32} = 10 + v_{32}$	0	10	4	14	2	12
(3, 4)	$t_{34} = 50 + v_{34}$	3	53	2	52	2.5	52.5
Path							
1-3-4		3	83	0	92	1.5	87.5
1-3-2-4		0	70	4	94	2	82
1-2-3-4		0	106	2	106	1	106
1-2-4		3	83	0	92	1.5	87.5

Table 2-2 displays two BRUE flow distributions, BRUE-1 and BRUE-2. The maximum differences between the lengths of utilized paths and the shortest paths are 13 for BRUE-1 and 14 for the other, i.e., both differences are within the threshold value. However, the convex combination of the two distributions 0.5×(BRUE-1 + BRUE-2) is not a BRUE flow distribution because the maximum difference now is 24. Thus, the set of BRUE flows is not convex. This non-convexity is largely due to the nonlinear condition (2.2). Similarly, the restrictive link-based BRUE set is not convex either due to the condition (2.7).

2.2.3 Finding Best- and Worst-Case BRUE Flow Distributions

In practice, traffic assignment models in the four-step process are based on PRUE and typically provide a unique equilibrium solution. In other words, PRUE models typically provide a point estimate of traffic flow distribution. On the other hand, there are generally many BRUE flow distributions and models based on BRUE provide an interval estimate instead.

To illustrate, the two problems below find BRUE flow distributions with the best or worst travel delay. To avoid generating paths, the problems use the more restrictive link-based BRUE conditions, instead of the more general path-based conditions (2.1)-(2.5). The formulation contains auxiliary variables, z_{ij}^{w}, and additional constraints to highlight the complementarity structure in the problems.

BC/WC-BRUE:

$$
\begin{aligned}
&\min_{(v,x,\varepsilon,\pi,\mu)}/\max && t(v)^T v && \\
&\text{s.t.} && x_{ij}^w z_{ij}^w = 0 && \forall w \in W,\ (i,j) \in L \\
& && z_{ij}^w \geq \varepsilon_{ij}^w - (\mu_i^w - \mu_j^w) && \forall w \in W,\ (i,j) \in L \\
& && z_{ij}^w \geq 0 && \forall w \in W,\ (i,j) \in L \\
& && (2.6), (2.8) – (2.11) &&
\end{aligned}
$$

The above problems are MPCC, a class of optimization problems difficult to solve because the problems are generally non-convex and violate the Mangasarian-Fromovitz constraint qualification (MFCQ) at any feasible point (see, e.g., Scheel and Scholtes, 2000). In the literature, many (see, e.g., Luo et al. 1996 and references cited therein) have proposed special algorithms to solve MPCC. Lawphongpanich and Yin (2010) applied concepts from manifold suboptimization and proposed a new algorithm that converges to a strongly stationary solution in a finite number of iterations. The algorithm can be applied with multiple initial solutions to solve both formulations for good strongly stationary solutions.

2.2.4 Numerical Examples

This subsection presents two numerical examples to demonstrate the relevance of BRUE. BC-BRUE and WC-BRUE are solved on two networks: nine-node (see, e.g., Hearn and Ramana, 1998) and Sioux Falls (see, e.g., LeBlanc et al., 1975) using GAMS (Brook et al, 2003) and CONOPT (Drud, 1995).

Nine-node problem: Figure 2-3 displays the underlying network. The network data can be found in Hearn and Ramana (1998). There are four O-D pairs and the demands are $q^{1-3} = 10$, $q^{1-4} = 20$, $q^{2-3} = 30$ and $q^{2-4} = 40$. The threshold value is assumed to be $\bar{\varepsilon}^w = \alpha \cdot t_{PRUE}^{*w}$ where α is a parameter and t_{PRUE}^{*w} is the PRUE travel time between a given O-D pair *w*.

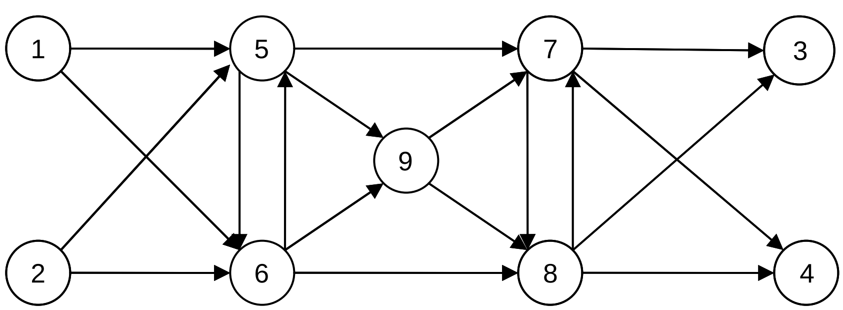

Figure 2-3. The nine-node network

Results for the nine-node problem are presented below. Table 2-3 compares the PRUE, system optimum (SO), best- and worst-case BRUE flow distributions with $\alpha = 0.10$. Figure 2-4 displays the system travel times of SO, best- and worst-case BRUE flow distributions with α varying from 0 to 0.20. When $\alpha = 0$, the BRUE flow distribution reduces to the unique PRUE distribution and there is no difference between the best- and worst-case performances. As α increases, the difference becomes more substantial. For example, the difference (measured as a percentage of the best-case system travel time) rises from 9.2 percent to 21.0 percent when α changes from 0.10 to 0.20. As the SO flow distribution is still the one that minimizes total system travel time, it does not change with the threshold value. In fact, the total travel time associated with SO always provides a valid lower bound for the best-case BRUE performance. As evident in Figure 2-4, the quality of SO bound is acceptable when α is large. On the other hand, the upper bound for the worst-case BRUE performance is more difficult and time-consuming to obtain and is one of our topics for further investigation.

Table 2-3. Flow Distributions for the Nine-Node Network ($\alpha = 0.10$)

Link	PRUE	WC-BRUE	BC-BRUE	SO
(1, 5)	8.2	4.0	11.5	9.4
(1, 6)	21.8	26.0	18.5	20.6
(2, 5)	47.4	53.2	43.0	38.3
(2, 6)	22.6	16.8	27.0	31.7
(5, 6)	0.0	0.0	0.0	0.0
(5, 7)	27.8	29.2	26.4	21.3
(5, 9)	27.7	28.0	28.0	26.4
(6, 5)	0.0	0.0	0.0	0.0
(6, 8)	44.5	42.8	45.6	39.5
(6, 9)	0.0	0.0	0.0	12.8
(7, 3)	38.2	34.0	31.7	29.6
(7, 4)	17.4	23.2	22.8	20.8
(7, 8)	0.0	0.0	0.0	0.0
(8, 3)	1.8	6.0	8.3	10.4
(8, 4)	42.6	36.8	37.2	39.2
(8, 7)	0.0	0.0	0.0	0.0
(9, 7)	27.7	28.0	28.0	29.1
(9, 8)	0.0	0.0	0.0	10.2

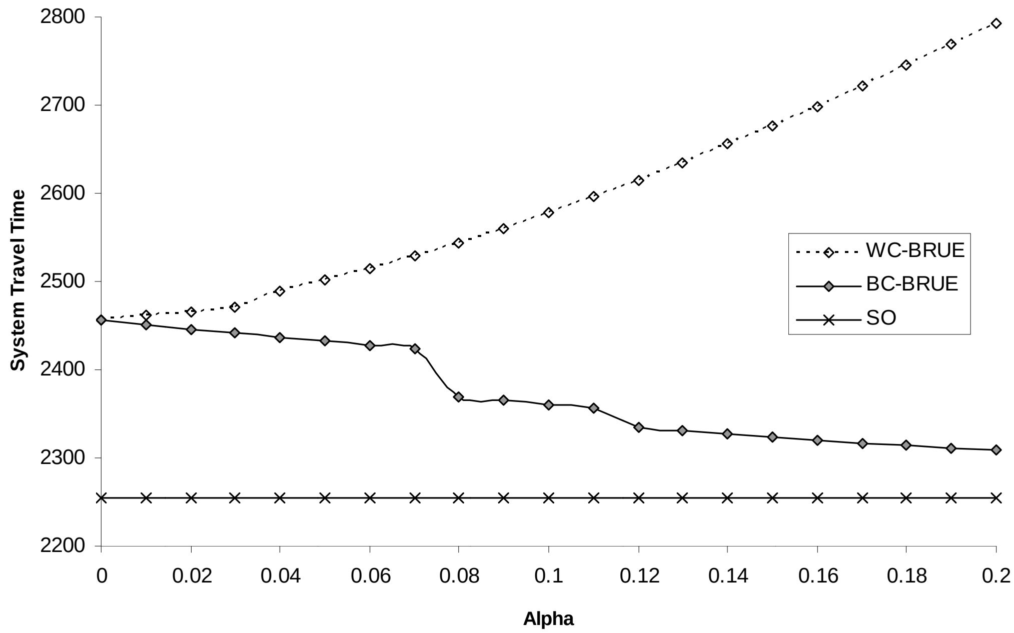

Figure 2-4. Comparison of system performances of BRUE at the nine-node network

Sioux Falls problem: The Sioux Falls network (see, LeBlanc et al., 1975) contains 76 links, 24 nodes and 528 O-D pairs. The original network parameters in LeBlanc et al (1975) are used while original demands are divided by 11. We assume the same threshold value for users departing from the same origin, i.e., $\bar{\varepsilon}^o = \alpha \cdot \tilde{t}^o_{PRUE}$ where $\tilde{t}^o_{PRUE}$ is the maximum PRUE travel times among the O-D pairs that share the same origin o.

Figure 2-5 presents the difference between the best and worst system performances of BRUE flow distributions for Sioux Falls with α varying from 0 to 0.20. Although not congested, the differences in the two system performances for Sioux Falls have characteristics similar to those of the nine-node network. For Sioux Falls, the difference in the two system performances increases up to 6.7 percent.

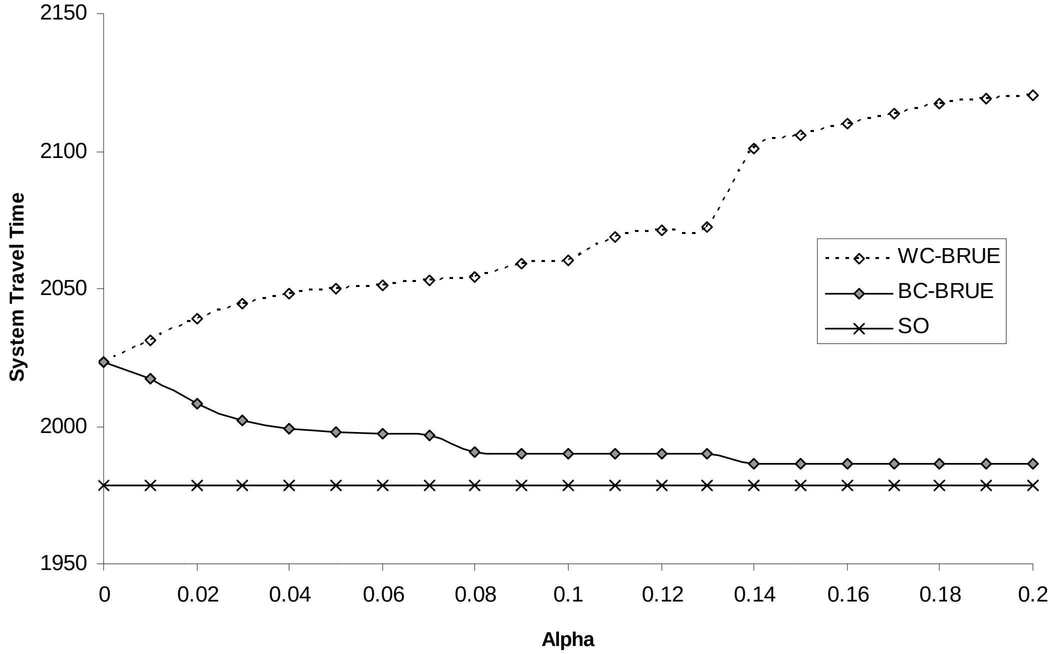

Figure 2-5. Comparison of system performances of BRUE at the Sioux Falls network

The above two examples reveal a difficulty of evaluating or designing improving strategies to highway networks as the resulting performances are likely to be uncertain (Mahmassani and Chang, 1987). Such uncertainty should be accommodated proactively in the decision-making process. The true range of possible total system travel times may be larger than, e.g., those shown in Figures 2.4 and 2.5, for two reasons. First, the link-based conditions (2.6) – (2.11) only characterize a subset of BRUE flows. Second, the algorithms we implemented, like most algorithms for MPCC, do not guarantee local or global optimality, regardless of the fact that we initiated or "warm-started" the algorithms with many initial solutions, randomly generated and otherwise.

2.3 CONGESTION PRICING WITH BOUNDEDLY RATIONAL USER EQUILIBRIUM

2.3.1 Model Formulations

To motivate the models, we implement a traditional MC pricing scheme on the nine-node network. Under the MC pricing, tolls are in the form of $t_{ij}^{'}(v_{ij}^{SO})\cdot v_{ij}^{SO}$ where v_{ij}^{SO} is the SO flow. Imposing such a pricing scheme may not necessarily evolve the system to SO, because the tolled BRUE flow distributions are generally not unique. Figure 2-6 presents the best and worst performances that the MC pricing scheme may achieve as compared with those without pricing. As expected, the MC pricing may result in a range of system performance and the difference can be as high as 21.3 percent when $\alpha = 0.20$. Although the MC pricing achieves SO under the best scenario (i.e., the scenario with perfect rationality), it may potentially make the traffic condition worse because users are not perfectly rational. When α is greater than 0.08 in Figure 2-6, the worst-case system travel time with the MC pricing is greater than the best-case travel time without tolling.

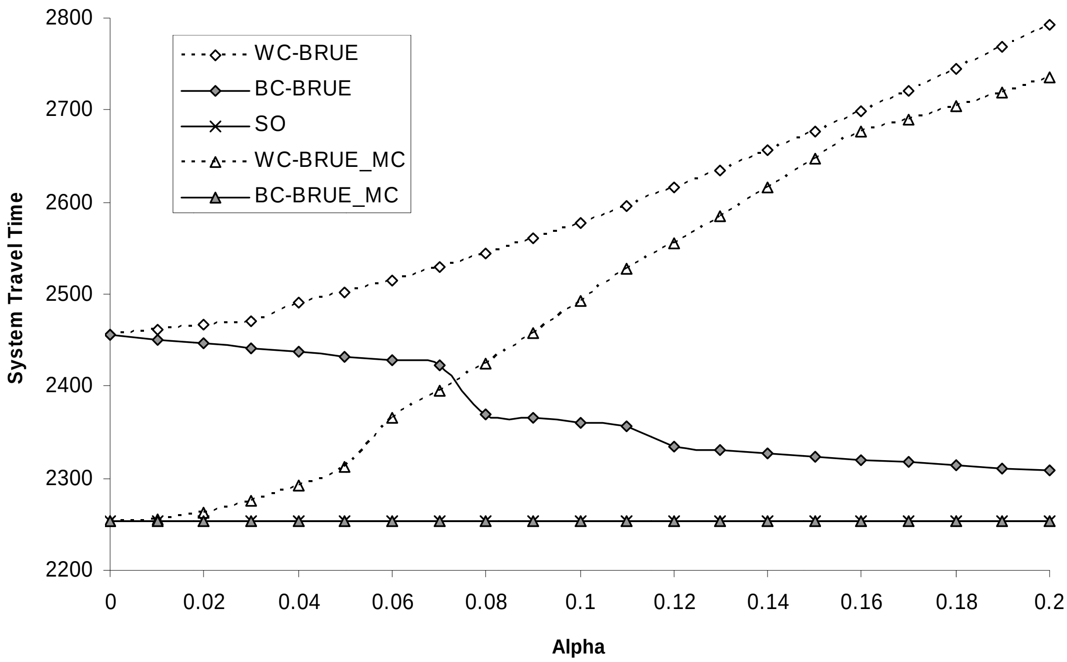

Figure 2-6. System performances with MC pricing scheme at the nine-node network

Although Figure 2-6 does not show a case that the MC pricing leads to an inferior worst-case performance, we do observe it when α is large. This suggests that the MC pricing does not necessarily ensure an improvement in the worst-case performance. Consider a network with three parallel links connecting one O-D pair in Figure 2-7. Assume that the O-D demand is 2 and the threshold value is 3. It is easy to verify that the worst-case BRUE flow distribution is $v = (2,0,0)$, with a total system travel time of 8. The SO flow for the problem is $v^{SO} = (1,0,1)$. This yields the MC toll $\tau^{MC} = (2,0,1)$. The worst-case BRUE flow distribution with MC tolls is $(0,2,0)$ and has a system travel time of 10, an amount larger than the one without any toll.

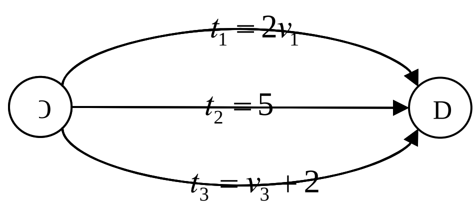

Figure 2-7. Three-parallel-link network

In real-world applications, decision-makers and planners tend to be risk-averse and may be more concerned with the worst-case performance. Following the notion of robust optimization (e.g., Ben-Tal and Nemirovski, 2002), we attempt to determine a pricing scheme to minimize the worst-case system travel time among all the tolled BRUE distributions. Then, the problem of finding an optimal pricing scheme can be formulated as the following min-max program:

RTP-1: $\min_{\tau} \max_{(v,x,\varepsilon,\pi,\mu)} \quad t(v)^T v$

$$\text{s.t.} \quad t_{ij}(v_{ij}) + \tau_{ij} - \varepsilon_{ij}^w + \pi_i^w - \pi_j^w = 0 \qquad \forall w \in W,\ (i,j) \in L \tag{2.15}$$

$$0 \le \tau \le \tau_{\max} \tag{2.16}$$

$$(2.7)\text{-}(2.11)$$

where, τ denotes a toll vector with a link toll τ_{ij} as its element and $\tau_{\max}$ is the maximum toll vector that can be possibly charged to each link.

For convenience, we represent the feasible region of the inner problem or the maximization part of RTP-1 as $\Xi(\tau)$, the decision variable $(v, x, \varepsilon, \pi, \mu)$ as ξ and thus the objective function as $\varphi(\xi)$. The inner problem can then be written as:

RTP-1-IN:
$$\psi(\tau) = \max_{\xi}\{\varphi(\xi) : \xi \in \Xi(\tau)\} \tag{2.17}$$

It then follows that RTP-1 is essentially in a form of $\min_{0 \le \tau \le \tau_{\max}} \psi(\tau)$, which is a generalized semi-infinite min-max problem (see, e.g., Polak and Royset, 2005), because the feasible set of the inner problem depends on the decision variables of the outer problem. A generalized semi-infinite optimization problem is more difficult to solve than its ordinary counterpart (e.g., Lopez and Still, 2007). There are only a few studies dealing with numerical algorithms for such a generalized problem (see, e.g., Still, 1999), and the methods presented may not be applicable to RTP-1 as its inner problem is a MPCC and the MFCQ is not satisfied at any feasible point of $\Xi(\tau)$.

The optimum solution to RTP-1 is expected to reduce the worst-case system travel time but without any guarantee for its best-case performance. Alternatively, it may be meaningful to find a robust toll whose best-case performance is guaranteed. Recall that Hearn and Ramana (1998) derived a "valid" toll set for PRUE, which consists of an infinite number of valid tolls and each valid toll can evolve the SO distribution when users are perfectly rational. Clearly, any toll vector in Hearn and Ramana's valid toll set will achieve SO as its best-case performance under the BRUE setting. However, other toll vectors not in the valid toll set may also admit SO as their tolled best-case performance. We denote all these tolls as "optimistic" tolls.

We now derive the optimistic toll set. Let $S := \arg\min\{t(v)^T v \mid v \in V\}$ where

$V := \left\{ v \middle| \Delta v = \sum_w D^w \text{ and } v \ge 0 \right\}$ denotes the feasible aggregate link flow set, and

$X(v) := \left\{ x \middle| \sum_w x^w = v \text{ and } \Delta x^w = D^w, x^w \ge 0, \forall w \in W \right\}.$

Let τ be a toll vector, $\hat{v}$ be a feasible aggregate flow and $\hat{x} \in X(\hat{v})$. Let $\hat{x}$ be a tolled (link-based) BRUE flow distribution induced by the toll vector τ, i.e. there exist vectors $\rho^w \in R^{|N|}$, $\eta^w \in R^{|L|}$ and $\upsilon^w \in R^{|N|}$ such that the following holds:

$$t_{ij}(\hat{v}_{ij}) + \tau_{ij} - \eta_{ij}^w + \rho_i^w - \rho_j^w = 0 \qquad \forall w \in W,\ (i,j) \in L \tag{2.18}$$

$$\hat{x}_{ij}^w \left(-\eta_{ij}^w + \upsilon_i^w - \upsilon_j^w \right) \ge 0 \qquad \forall w \in W,\ (i,j) \in L \tag{2.19}$$

$$-\upsilon_{d(w)}^w \le \bar{\varepsilon}^w - \upsilon_{o(w)}^w \qquad \forall w \in W \tag{2.20}$$

$$\eta_{ij}^w \ge 0 \qquad \forall w \in W,\ (i,j) \in L \tag{2.21}$$

In the above, the triplet (ρ, η, υ) plays the role of (ε, π, μ) in the link-based BRUE conditions (2.6) – (2.8). More specifically, ρ, η, υ are vectors of node potentials associated with travel time, travel times in excess of the minimum, and node potentials associated with the excess travel times respectively in the tolled BRUE.

Theorem 3.1: Let $T(\hat{x})$ denote the τ part of the polyhedron (2.18) – (2.21), then the optimistic toll set is equivalent to $\mathcal{T} := \bigcup_{v \in S} \left(\bigcup_{\hat{x} \in X(v)} T(\hat{x}) \right)$.

Proof:

Necessity: If τ is an optimistic toll, then there must exist some feasible commodity (O-D pair) link flow $\hat{x}$ in the tolled BRUE flow set whose aggregate link flow $\hat{v}$ is SO, i.e. $\tau \in T(\hat{x})$. Together with that $\hat{v} \in S$ and $\hat{x} \in X(\hat{v})$, we have $\tau \in \mathcal{T}$.

Sufficiency: If $\tau \in \mathcal{T}$, τ must belong to some set $T(\hat{x})$ where the aggregate link flow corresponding to $\hat{x}$ is the SO flow. Therefore, $\hat{x}$ is a tolled link-based BRUE flow with τ being the toll vector; and τ is an optimistic toll since the tolled best-case BRUE can achieve SO. □

The optimistic toll set $\mathcal{T}$ is not necessarily convex although all its component sets *T* are polyhedrons. Even when the set *S* is singleton under the assumption that the link travel time function is strictly monotone, set $\mathcal{T}$ is still a union of an infinite number of subsets *T* because the commodity link flow will not be unique. When there is only one commodity, the optimistic toll set $\mathcal{T}$ reduces to a polyhedron. As previously indicated, Hearn and Ramana's valid toll set is a subset of the optimistic toll set $\mathcal{T}$.

All optimistic tolls achieve SO at their best-case performance, but their worst-case performances are not necessarily the same. We then formulate an alternative model to find the most robust toll vector from the optimistic toll set. The solution will achieve SO at its best-case performance but probably lead to a higher worst-case travel time compared with the solution to RTP-1. Since $\mathscr{T}$ is a complicated set, we instead use its subset, the valid toll set in Hearn and Ramana (1998), in formulating the robust toll problem for a proof of concept. With the assumption of strictly monotonic link travel time functions, S is singleton. The alternative robust pricing problem can be formulated as follows:

RTP-2: $\min\limits_{(\tau,\rho)} \quad \psi(\tau)$

$$\text{s.t.} \quad v^{SO^T}\left(t\left(v^{SO}\right)+\tau\right)+\sum_w D^{w^T}\rho^w = 0 \tag{2.22}$$

$$t_{ij}\left(v_{ij}^{SO}\right)+\tau_{ij}+\rho_i^w-\rho_j^w \geq 0 \qquad \forall w\in W,\ (i,j)\in L \tag{2.23}$$

As formulated, RTP-2 is another generalized semi-infinite min-max problem, which is of the same complexity as RTP-1. The inner problems are the same, defining the worst-case tolled BRUE flow distribution, as shown in (2.17). The former incorporates some additional linear constraints (2.22) – (2.23) in its outer problem, which are separable from its inner problem. The linear constraints define the valid toll set (Hearn and Ramana, 1998), and ensure that SO flow satisfies the tolled PRUE conditions with τ being the toll vector and ρ the corresponding node potentials. Consequently, SO flow will be a tolled BRUE flow distribution induced by the toll vector τ, i.e., the toll achieves SO at its best-case performance.

2.3.2 Solution Algorithm

We propose a heuristic procedure to solve RTP-1 and RTP-2. The key idea is to use a differentiable penalty function to remove the constraints of the inner problem involving the decision variables of the outer problem, thereby transforming a generalized semi-infinite min-max problem into an ordinary semi-infinite optimization problem. The procedure then applies a cutting-plane scheme (e.g., Lawphongpanich and Hearn, 2004) to solve a sequence of ordinary finite optimization problems, each one better approximating the original problem than its predecessors. In the following, we use solving RTP-1 as an example to describe the procedure.

We formulate a penalized inner problem as follows:

P-WS(τ): $\max\limits_{(v,x,\varepsilon,\pi,\mu)} \quad t(v)^T v - M\sum_w\sum_{ij}(t_{ij}+\tau_{ij}-\varepsilon_{ij}^w+\pi_i^w-\pi_j^w)^2$

s.t. (2.7)-(2.11)

where M is a sufficiently large penalty parameter. For convenience, we further denote the feasible region of the above problem as Ω and then the objective function as $\hat{\varphi}(\xi,\tau)$. With a finite penalty, P-WS(τ) provides an upper bound to the original inner problem. Given a toll vector τ, assume that $\bar{\xi}$ is the optimal solution to the original problem RTP-1-IN, and let $\hat{\xi}$

denote the optimal solution to the above penalized problem for some M > 0. It follows that $\varphi(\bar{\xi}) = \hat{\varphi}(\bar{\xi},\tau) \le \hat{\varphi}(\hat{\xi},\tau)$. The first equality is due to that no penalty is associated with $\bar{\xi}$ and the second inequality is due to the fact that $\bar{\xi}$ is feasible to the penalized problem. As M goes to infinity, P-WS(τ) reduces to the original inner problem.

We then formulate a penalized version of robust toll problem RTP-1 as $\min_{0\le\tau\le\tau_{\max}} \max_{\xi\in\Omega} \hat{\varphi}(\xi,\tau)$. Because the objective is to minimize the upper bound of total system travel time, the solution may reduce the worst-case system travel time as the upper bound is pretty tight when the penalty parameter is sufficiently large. Note that the penalized robust optimization problem is an ordinary semi-infinite min-max problem because the feasible region of its inner problem does not depend on the decision variables of the outer problem. Moreover, it is equivalent to the following ordinary semi-infinite optimization problem:

$$
\begin{aligned}
\text{P-RTP-1} \quad & \min_{(\tau,\varpi)} && \varpi \\
& \text{s.t.} && \varpi \ge \hat{\varphi}(\xi,\tau) && \forall \xi \in \Omega \\
& && 0 \le \tau \le \tau_{\max}
\end{aligned}
$$

We now discuss a cutting-plane scheme to solve P-RTP-1. Assume that ξ^1, ξ^2, …, ξ^n are elements of Ω. Then, a relaxed penalized robust toll problem (RP-RTP-1) can be written as:

$$
\begin{aligned}
\text{RP-RTP-1} \quad & \min_{(\tau,\varpi)} && \varpi \\
& \text{s.t.} && \varpi \ge \hat{\varphi}(\xi^i,\tau) && \forall i = 1,\dots,n \\
& && 0 \le \tau \le \tau_{\max}
\end{aligned}
$$

The RP-RTP-1 problem stated above is simply the original P-RTP-1 problem with Ω approximated by the discrete set $\overline{\Omega}$={ξ^1, …, ξ^n}. Let $(\tilde{\tau},\tilde{\varpi})$ be a global optimal solution to the above relaxed toll problem. If $(\tilde{\tau},\tilde{\varpi})$ is feasible to the original P-RTP-1 problem, it is an optimal solution. To check its feasibility, one may solve P-WS($\tilde{\tau}$), i.e., $\max_{\xi\in\Omega} \hat{\varphi}(\xi,\tilde{\tau})$. If $\tilde{\xi}$, a global optimal solution to P-WS($\tilde{\tau}$) is such that $\hat{\varphi}(\tilde{\xi},\tilde{\tau}) \le \tilde{\varpi}$, then $(\tilde{\tau},\tilde{\varpi})$ is an feasible and optimal solution to P-RTP-1. On the other hand, if $\hat{\varphi}(\tilde{\xi},\tilde{\tau}) > \tilde{\varpi}$, then an improved solution may be obtained by solving the RP-RTP-1 problem with an expanded discrete set $\overline{\Omega} \cup \{\tilde{\xi}\}$.

Below is a detailed description of the procedure we outlined above:

Step 0: Solve the WC-BRUE problem without tolls to obtain an initial solution ξ^1. Set

$n = 1$ and $\overline{\Omega}^1 = \{\xi^1\}$.

Step 1: Solve the RP-RTP-1 problem with the discrete set $\overline{\Omega}^n$ and let (τ^n, ϖ^n) denote the resulting optimal solution.

Step 2: Solve P-WS(τ^n) and let $\xi^{(n+1)}$ denote the resulting optimal solution.

Step 3: If $\hat{\varphi}(\xi^{(n+1)}, \tau^n) \le \varpi^n$, stop and τ^n is an optimal robust pricing scheme. Otherwise, set $\overline{\Omega}^{(n+1)} = \overline{\Omega}^n \cup \{\xi^{(n+1)}\}$ and $n = n + 1$. Go to Step 1.

Assume that both (τ^n, ϖ^n) and $\xi^{(n+1)}$ globally solve the RP-RTP and P-WS(τ^n) problems in Steps 1 and 2, respectively. If the above algorithm stops at some finite iteration *n*, it is easy to see that (τ^n, ϖ^n) is an optimal solution to the original P-RTP problem. When the algorithm generates an infinite sequence, any of its subsequential limits is optimal to the P-RTP-1 problem under a set of strong conditions discussed in Yin and Lawphongpanich (2007). Because it is difficult in practice to verify those conditions and ensure global optimality for solving RP-RTP-1 and P-WS(τ^n) problems, the above algorithm should be regarded as heuristic in general.

2.3.3 Numerical Examples

The above algorithm was implemented using GAMS to solve both RTP-1 and RTP-2 for the nine-node network. We set *M* to 10,000 based on preliminary results and the upper bound for the toll on each link to the minimum integer number that is greater than the MC toll. Other problems parameters are the same as in Section 2.2.4. RTP-1 was solved with $\alpha = 0.05$, 0.10, 0.15 and 0.20 while RTP-2 was solved with $\alpha = 0.20$ for comparison purpose.

Since the outer problem is a nonconvex quadratic program and the inner problem is a MPCC, multiple (10 and 4 respectively) initial solutions were used in Step 2 and 3 in order to obtain better local optimal solutions. The computation time thus increased significantly. Although not particularly efficient, the cutting-plane algorithm generated reasonable solutions. When $\alpha = 0.05$, the robust toll from solving RTP-1 was the same as the MC toll (reported in Table 2-4) while different tolls were obtained for the other three scenarios. Table 2-4 reports the robust toll vector for $\alpha = 0.20$, denoted as RT1.

Table 2-4. Pricing Schemes and Their Performances for the Nine-Node Network

Link	No Toll	MC Toll	RT1	RT2
(1, 5)	-	1.13	0.00	2.00
(1, 6)	-	6.16	4.43	6.00
(2, 5)	-	2.59	0.00	0.00
(2, 6)	-	3.62	4.00	0.00
(5, 6)	-	0.00	1.00	1.00
(5, 7)	-	16.88	17.00	15.81
(5, 9)	-	5.13	4.37	4.61
(6, 5)	-	0.00	0.00	1.00
(6, 8)	-	7.37	2.42	7.81
(6, 9)	-	0.11	1.00	0.61
(7, 3)	-	3.54	0.00	4.00
(7, 4)	-	2.01	0.00	3.00
(7, 8)	-	0.00	1.00	1.00
(8, 3)	-	0.02	0.00	0.00
(8, 4)	-	2.50	0.00	3.00
(8, 7)	-	0.00	1.00	1.00
(9, 7)	-	3.75	4.00	3.20
(9, 8)	-	0.06	1.00	0.00
Best-case system travel time	2309	2254	2306	2254
Worst-case system travel time	2793	2735	2509	2662

Figure 2-8 compares the worst-case total travel time with robust tolls resulting from RTP-1 (RT in the figure), the MC toll and no toll (NT in the figure). When compared to the situation with no toll, the figure shows that robust tolls reduce the worst-case system travel time significantly, e.g., the reduction is approximately 10.2 percent when $\alpha = 0.20$. When compared to MC tolls, robust tolls have superior worst-case performances when α is large, in particular when $\alpha \geq 0.05$. For smaller α, BRUE does not deviate much from PRUE, thereby implying that the worst-case performances of robust and MC tolls are similar.

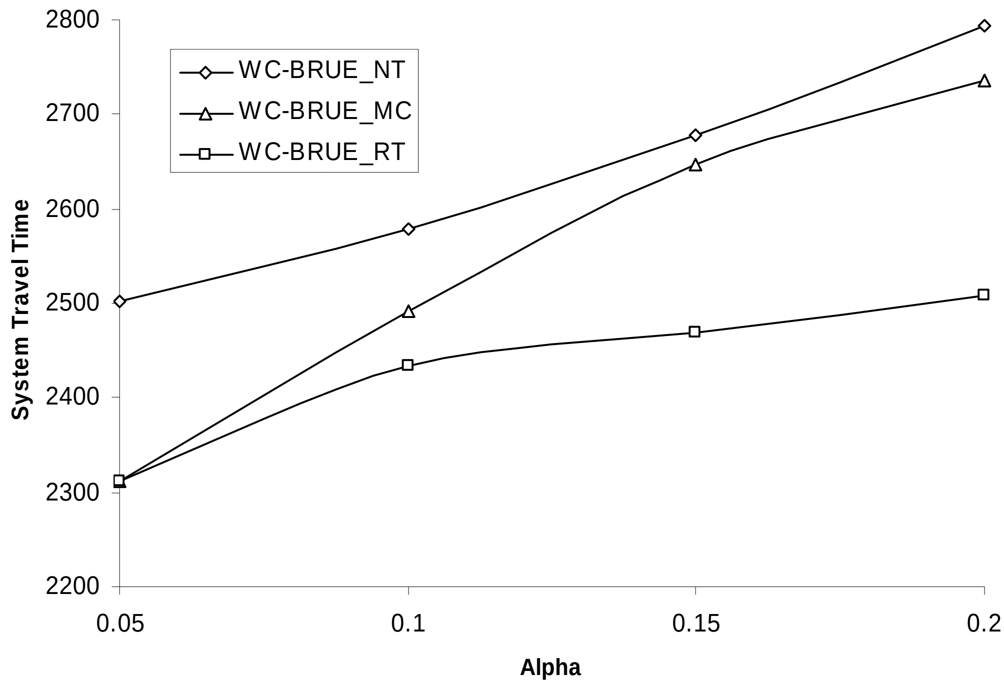

Figure 2-8. Comparison of worst-case total travel times with no toll, robust and MC tolls at the nine-node network

The solution to RTP-2 with $\alpha = 0.20$ is also reported in Table 3.2, denoted as RT2. Table 3.2 also presents the best- and worst-case system travel times of MC, RT1 and RT2 with $\alpha = 0.20$. From the table, RT2 achieves SO at its best-case performance while reducing the worst-case system travel time from 2793 to 2662, a 4.7 percent reduction. If the full set of optimistic tolls is considered, a higher reduction rate can be expected. RT2 also dominates MC in the sense that both tolls have the same best-case performances while the former performs better against the worst-case scenarios.

The parameter α reflects the level of rationality in travelers' route choice decision making, which can be estimated by conducting a stated preference survey. However, given the fact that the estimate of α can be biased or inaccurate, it makes sense to examine how a robust toll designed for one particular level of rationality performs at other levels of rationality. In Figure 2-9, tolls from RTP-1 with $\alpha = 0.20$ (denoted as RT1) reduces both the best- and worst-case system travel times significantly for all α values compared with the no-toll case. Compared with the MC toll, the same toll leads to a superior worst-case performance with $\alpha \geq 0.08$ but inferior otherwise. Intuitively, the smaller α is, the more rational travelers' route choices are. Thus the first-best tolls are expected to perform well with small α values.

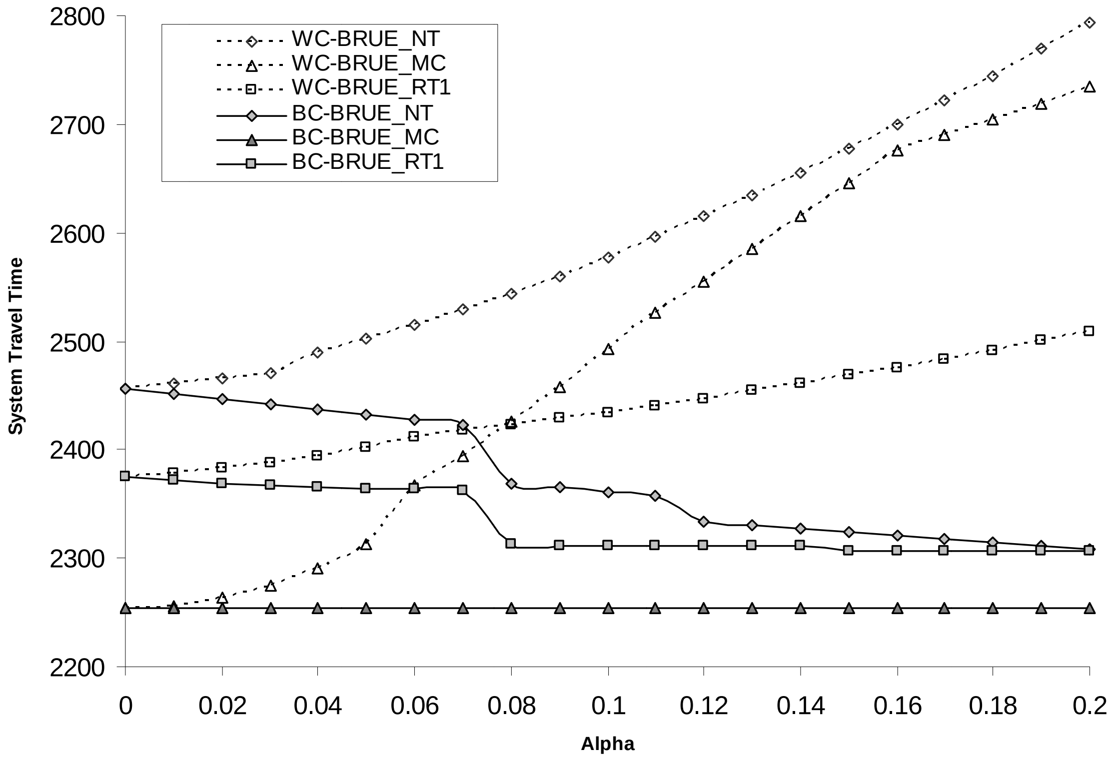

Figure 2-9. System performances with MC and RT1 at the nine-node network

We further note that although robust tolls are designed to guard against the worst-case scenarios, implementation of robust tolls actually leads to a more stable system performance in the sense that the span between the best and worst performances is much narrower. Figure 2-10 displays the difference between the worst- and best-case travel time as a percentage (or fraction) of the latter. In all three cases (no toll, MC and RT1 tolls), the difference increases as α increases. However, the difference for the case with the robust toll (see the bottom most graph) is significantly smaller than the other two for large α. This suggests that there is less variability in travel time under robust tolls, i.e., the tolls are more effective and reliable at inducing travelers to use the road network more efficiently, especially when the threshold value is relatively large.

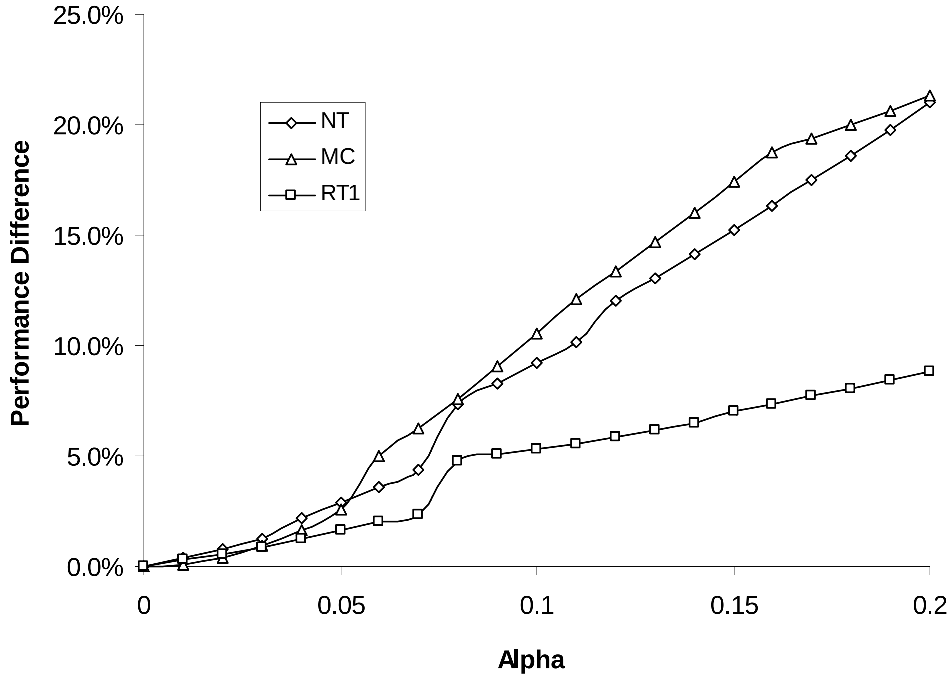

Figure 2-10. System performances with MC and RT1 at the nine-node network

3. PRICING STOCHASTIC NETWORKS

3.1 INTRODUCTION

Recognizing that traffic condition is intrinsically stochastic, this chapter considers stochastic networks where travel times are assumed to be probabilistic and the outcome of travelers' route choice is thus uncertain. As before, the demand remains deterministic. In the literature, some have attempted to model how travelers behave in such an uncertain traffic environment. The proposed models include, among others, the expected-utility-theory-based models (e.g., Mirchandani and Soroush, 1987; Yin and Ieda, 2001), the travel-time-budget models (e.g., Lo et al. 2006; Shao et al., 2006), the late-arrival-penalty model (Walting, 2006), and the mean-excess-travel-time model (e.g., Zhou and Chen, 2008). However, most of the models assume perfect rationality and none has investigated how to price a stochastic network.

This chapter presents an alternative user equilibrium model for stochastic traffic networks based on the cumulative prospect theory (CPT, Tversky and Kahneman, 1992). Advanced by psychologists and behavioral economists, CPT provides a well-supported descriptive paradigm for decision-making under risk or uncertainty. A variety of phenomena and experimental data in the transportation context, which cannot be explained by the expected utility theory previously, have been well explained by CPT (e.g., Avineri and Prashker, 2003; Bogers and Zuylen, 2004). In recent years, CPT has been applied to model travelers' choices of departure times (e.g., Fujii and Kitamura 2004; Jou et al., 2008), routes (e.g., Avineri and Prashker, 2004; Viti et al., 2005), bus lines (Avineri, 2004) and others (e.g., Schwanen and Ettama, 2009). Avineri (2006) was the first to incorporate CPT in the equilibrium analysis of stochastic networks, and Connors and Sumalee (2009) presented a general prospect-based user equilibrium model for stochastic networks, which was further tailored into the case with endogenous stochastic demand and supply (Sumalee et al., 2009). These previous studies emphasize the strong influence of reference points on the resulting flow pattern. However, both studies rely on exogenous inputs of reference points, and no guidance was provided on how the values are derived.

Reference points are important parameters in CPT. In the context of route choice, with respect to a reference point (time), the realized payoff of a path is framed into either a gain or loss and its travel prospect can be subsequently determined. Previous studies (e.g., Avineri and Prashker, 2004) show that travelers will choose paths with maximal prospects. It is thus apparent that the locations of reference points have a strong influence on the flow pattern. The prospect-based user equilibrium models with exogenous reference points cannot be applied without estimating the reference points beforehand. This implies that the resulting reference-dependence could be regarded as an ad hoc assumption (for discussions in other domains, see, e.g., Pesendorfer, 2006; Koszegi and Rabin, 2003; Schmidt et al., 2008 and Schmidt and Zank, 2010.) Moreover, according to Munro and Sugden (2003), evidence shows that individuals adjust their reference points quickly in response to changes in their endowments. In the context of route choices, a traveler selects a route in accordance with one reference point.

The outcome of his or her travel may induce a change in the reference point, which may lead to further adjustment in his or her route choice, and so on. Therefore, a model with endogenous reference points is more competent to predict the long-run user equilibrium flow pattern.

This chapter presents a multiclass prospect-based user equilibrium model with endogenous reference points for stochastic networks where travel times are random and their distributions are assumed to be known to travelers. It is further assumed that travelers of each class have a desired on-time arrival probability and develop a capability of budgeting a time to achieve the probability through their past travel experiences (e.g., Lo et al., 2006). The budgeted time reflects the travelers' probabilistic belief they hold in their past experiences on travel times and can thus potentially serve as a reference point (e.g., Koszegi and Rabin, 2003). More specially, when they depart from their origin, travelers use the budgeted time as a reference point to determine the gain or loss of each path based on its travel time distribution, and make their route choices accordingly. A long-run user equilibrium will be achieved when no traveler can improve his or her travel prospect by unilaterally changing routes. In this state, the reference points will remain constant and are consistent with the resulting prospect-based user equilibrium flow pattern and the corresponding travel time distributions.

For the remainder, Section 3.2 describes basic assumptions of the model, introduces the computation of travel prospect value using CPT and then presents a descriptive model to determine travelers' reference points. Section 3.3 establishes the prospect-based use equilibrium conditions and formulates them as a variational inequality. Section 3.4 proposes a heuristic solution algorithm and then presents two numerical examples to demonstrate the proposed model and algorithm. In Section 3.5, a behaviorally consistent pricing model is developed to determine the optimal pricing scheme for stochastic networks. A numerical example is provided to illustrate the proposed model.

3.2 BASIC CONSIDERATIONS

3.2.1 Network Representation and Assumptions

Define $G = (N, A)$ as a strongly connected transportation network with N and A being the sets of nodes and links respectively. *Note that the notations of this chapter are different from those in the previous chapter*. Let R be the set of origin-destination (O-D) pairs and q_r represent travel demand for O-D pair $r \in R$. Let K_r be the set of paths for O-D pair r ("path" and "route" are used interchangeably in this chapter). For each path $k \in K_r$, f_r^k denotes the corresponding path flow. We further use v_a to denote the flow on link $a \in A$ and v is a vector of link flows of all links with v_a as its elements. More specifically, $v = \left(v_1, \cdots v_a, \cdots v_{|A|}\right)^T$, where $|\bullet|$ denotes the cardinality of a set. The path flows are related to the link flows by $v_a = \sum_{r\in R} \sum_{k\in K_r} \delta_{a,r}^k f_r^k$ where $\delta_{a,r}^k$ is a link-path incidence whose value is 1 if link a is on path k, and 0 otherwise. Similarly we use f to denote a vector of flows of all paths with f_r^k as its elements.

Let T_r^k denote the stochastic travel time of path k between O-D pair r and T is a vector of travel times of all paths. It is assumed that the joint probability density function of path travel times T is known, which is parameterized by link flows v (i.e., the functional form itself is independent of link flows.) We further denote the marginal cumulative distribution function of T_r^k as ψ_r^k, which is also parameterized by v (and thus f). It is noted that the distribution function may be parameterized by v in a very general sense (Walting, 2006) and two major factors may contribute to its functional form: stochastic capacity (e.g., Lo et al., 2006) and stochastic demand (e.g., Zhou and Chen, 2008; Lam et al., 2008). In the situations where the O-D demands or path and link flows are random variables, the corresponding notations introduced above represent their mean values. For example, the marginal cumulative distribution function ψ_r^k will be parameterized by the average link flows. We further assume that travelers know the travel-time distributions, and they are homogenous in all aspects except that they may possess different desired on-time arrival probabilities.

3.2.2 Travel Prospect Values

Given that CPT provides a well-supported descriptive paradigm for individuals' decision-making under risk or uncertainty, this chapter adopts the theory to describe travelers' route choices in stochastic networks. In a nutshell, CPT retains the framework of the expected utility theory but incorporates the following features that have been observed in numerous behavioral experiments:

i) People distinguish gains from losses before making choices. The payoffs are framed as gains or losses as compared to some reference points (e.g., Kahneman and Tversky, 1979).

ii) The loss looms larger than the gain, i.e., people generally care more about potential losses than potential gains. At the same time, they are risk-averse over gains and risk-seeking over losses (e.g., Thaler et al., 1997).

iii) People tend to overweight extreme, but unlikely events. At the same time, they underweight "average" events (e.g., Camerer and Ho, 1994).

Consequently, CPT can be viewed as an extension to the expected utility theory with the following three modifications (Tversky and Kahneman, 1992):

i) Replacing the final wealth with payoffs relative to the reference point. As shown in (3.1), the outcomes (x) are converted into gains ($\Delta x \geq 0$) or losses ($\Delta x < 0$) relative to a reference point (x_0).

$$\Delta x = x - x_0 \tag{3.1}$$

ii) Replacing the utility function with a value function to capture individuals' risk attitudes. The S-shaped value function, $g(x)$ in (3.2), is illustrated in Figure 3-1. The parameters α and β measure the degree of diminishing sensitivity of the value function. Typically, $0<\alpha,\ \beta<1$ and thus the value function exhibits risk aversion over gains and risk seeking over losses. The parameter $\eta \geq 1$ is called "loss-aversion" coefficient, indicating that individuals are more sensitive to losses than gains.

$$g(x)=\begin{cases}(x-x_0)^{\alpha}, & x \geq x_0 \\ -\eta(x_0-x)^{\beta}, & x<x_0\end{cases} \tag{3.2}$$

iii) Replacing cumulative probabilities with weighted cumulative probabilities. One typical inverse *S*-shaped weighting function is presented in (3.3) and further illustrated in Figure 3-2 where *p* is the cumulative probability level. The parameter γ represents the level of distortion in probability judgment in the decision-making process and $0<\gamma<1$.

$$w(p)=\frac{p^{\gamma}}{\left(p^{\gamma}+(1-p)^{\gamma}\right)^{1/\gamma}} \tag{3.3}$$

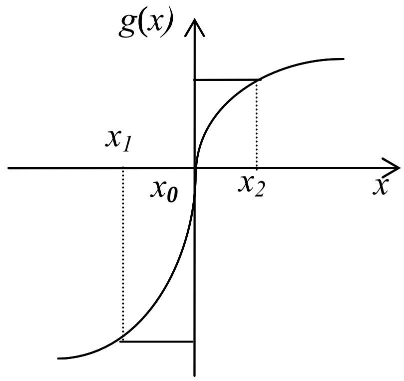

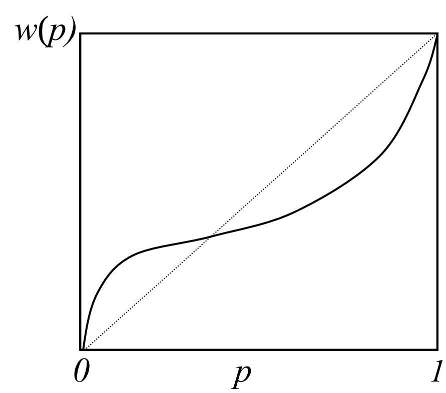

ion

With the above value and weighting functions, the prospect value of a decision with stochastic outcomes *x* can be written as:

$$PV=\int_{-\infty}^{x_0}\frac{dw(F(x))}{dx}g(x)dx+\int_{x_0}^{\infty}-\frac{dw(1-F(x))}{dx}g(x)dx \tag{3.4}$$

where PV is the prospect value and $F(x)$ denotes the cumulative distribution function (CDF) of the associated outcome *x*. Equation (3.4) is a straightforward generalization of the original discrete formulation proposed by Tversky and Kahneman (1992). See, e.g., Connors and

Sumalee (2009), for its derivation.

As demonstrated by previous studies (e.g., Katsikopoulos et al., 2002; Avineri and Prashker, 2004; Zhou et al., 2009), travelers behave as prospect maximizers and the above framework can be applied to represent their route choices under risk. More specifically, compared to a reference point, travelers may consider the outcome of a trip as a gain, if the travel time is less than the reference time; as a loss if otherwise. Moreover, they are observed to present a diminishing sensitivity with respect to gains and losses. For example, Zhou et al. (2009) calibrated the parameters of the value function for route choices. The calibrated values, α =0.37, β =0.59 and η =1.51 are consistent with the above observations.

We now consider a trip between O-D pair r with ϖ_r as the reference point. The relative payoff for choosing a path *k* can be defined as $\varpi_r - T_r^k$. Consequently, the prospect of path *k* can be calculated through (3.5) and (3.6).

$$g_r(x) = \begin{cases} (\varpi_r - x)^{\alpha}, x \le \varpi_r \\ -\eta(x - \varpi_r)^{\beta}, x > \varpi_r \end{cases} \tag{3.5}$$

$$U_r^k = \int_{\underline{t}_r^k}^{\varpi_r} \frac{dw((\psi_r^k(x))}{dx} g_r(x)dx + \int_{\varpi_r}^{\bar{t}_r^k} - \frac{dw(1-\psi_r^k(x))}{dx} g_r(x)dx \tag{3.6}$$

where *x* represents the path travel time; U_r^k is the prospect value of path *k* between O-D pair *r*; $\underline{t}_r^k$ and $\bar{t}_r^k$ are the lower and upper bounds of the travel time of path *k* respectively. In this chapter, the former is assumed to be the free-flow travel time and the latter is the 99.9999th percentile of the random travel time. Note that U_r^k is a function of *v* or *f*. Although travel times are stochastic, the travel prospects are deterministic.

Consistent with CPT, we assume that travelers base their route choices on the prospect values and always choose the path with the maximal U_r^k.

3.2.3 Reference Points

This section presents a conjecture on how the reference points are determined in the context of travelers' route choices.

We assume that the reference point for a traveler is the time he or she budgeted to ensure his or her desired on-time arrival probability. The latter depends on his or her trip purpose and risk-taking attitude. A low desired probability implies that either the trip is not important or the individual is risk seeking. Travelers are known to be capable of budgeting a longer travel time for a specific trip to hedge against travel time variability (e.g., Lo et al., 2006). The budgeted time reflects their probabilistic belief on travel times based on their preferences, and can thus potentially serve as reference points (e.g., Koszegi and Rabin, 2003).

Mathematically, suppose that a traveler has a desired on-time arrival probability of ρ, the budgeted time for taking path *k* of O-D pair *r*, i.e., ω_r^k, can be written as:

$$\omega_r^k = \min\{\omega \mid \Pr(T_r^k \le \omega) \ge \rho\} \tag{3.7}$$

With a continuous travel time distribution, taking the inverse of (3.7) leads to:

$$\omega_r^k = \zeta_r^k(\rho) \tag{3.8}$$

where $\zeta_r^k(\cdot)$ is the inverse function of $\psi_r^k(\cdot)$. Note that $\zeta_r^k(\cdot)$ is also parameterized by *v*. In other words, the budgeted time is the ρ th percentile of the travel time of path *k*.

It is assumed that through their past experiences, travelers develop a reference time for each O-D pair, the time they expect to reserve to guarantee a punctual trip. For route choice with fixed departure times, the reference time acts as a reference point to separate early arrivals (earlier than expected) from late ones (later than expected). Since there exist multiple paths between each O-D pair, the reference time is assumed to be a function of ω_r^k, i.e., the budgeted time for each path. One plausible assumption is that the reference time (point) is the minimum of the budgeted times of all paths, i.e.,

$$\varpi_r = \min_k\{\omega_r^k\} = \max\{\varpi \mid \zeta_r^k(\rho) \ge \varpi, \forall k \in K_r\} \tag{3.9}$$

Equations (3.7)–(3.9) are written for an individual traveler of O-D pair *r*. As aforementioned, travelers may possess different desired on-time arrival probabilities. Travelers of each O-D pair are thus grouped into *M* different classes with respect to their desired on-time arrival probabilities, denoted as ρ_r^j, $j = 1, \ldots, M$. These probabilities are exogenous variables and are not difficult to estimate in practice through surveys or interviews. Denote the reference point of each class as ϖ_r^j. Same as (3.9), ϖ_r^j is the solution of the following linear program:

$$\begin{aligned} &\max\ \varpi_r^j \\ &\text{s.t.}\quad \varpi_r^j - \zeta_r^k(\rho_r^j) \le 0, \quad \forall k \in K_r \end{aligned} \tag{3.10}$$

The above linear program always admits an (unique) optimal solution. Therefore, according to the strong duality theorem (see, e.g., Bertsimas and Tsitsiklis, 1997), it is equivalent to the following linear system:

$$1 - \sum_{k \in K_r} \lambda_r^{k,j} = 0$$

$$\varpi_r^j - \sum_{k\in K_r} \lambda_r^{k,j} \zeta_r^k(\rho_r^j) = 0$$
$$\lambda_r^{k,j} \ge 0\,, \quad \forall k \in K_r$$
$$\zeta_r^k(\rho_r^j) - \varpi_r^j \ge 0\,, \quad \forall k \in K_r$$

where $\lambda_r^{k,j}$ is the dual variable or the Lagrangian multiplier associated with (3.10).

Given a link flow pattern *v*, the parameterized ψ_r^k and ζ_r^k are determined. The ϖ part of the solution pair, i.e., (ϖ, λ), to the above system is the reference times (points). The prospect value for each class of users choosing path *k* between O-D pair *r*, denoted as $U_r^{k,j}$, can be computed via (3.5) and (3.6). Given that users will choose the paths with the maximal prospect, another link flow pattern, denoted as *v'*, can be determined. It is noted that the reference points determined above are based upon the link flow pattern *v*, and thus may not be consistent with the new link flow pattern *v'*. The points will be further adjusted and the next section presents a prospect-based user equilibrium model where the resulting reference points are consistent with the equilibrium flow pattern.

3.3. PROSPECT-BASED USER EQUILIBRIUM MODEL

3.3.1 Prospect-Based User Equilibrium

With the above consideration, a long-run user equilibrium will be achieved where for each class of travelers between each O-D pair, the travel prospect values of all utilized paths are equal, and are the same or greater than the prospect value of any unutilized path. No traveler can thus further increase his or her travel prospect by unilaterally changing routes. At equilibrium, travelers will stop adjusting their reference points, which remain constant and are consistent with the user equilibrium flow pattern and the corresponding travel time distributions.

Mathematically, the prospect-based user equilibrium conditions can be expressed as follows:

$$\begin{cases} f_r^{k,j} > 0 & U_r^{k,j} = \pi_r^j \\ f_r^{k,j} = 0 & U_r^{k,j} \le \pi_r^j \end{cases}, \quad \forall k \in K_r\,, \quad r \in R\,, \quad j = 1,\ldots,M \tag{3.11}$$

where $f_r^{k,j}$ is the flow on path *k* by traveler class *j* and $\pi_r^j = \max_{k\in K_r}\{U_r^{k,j}\}$.

3.3.2 Model Formulation

The above prospect-based user equilibrium conditions can easily be represented as the following nonlinear complementarity system. For completeness, we repeat some previously presented equations here.

$$f_r^{k,j}\left(\pi_r^j - U_r^{k,j}\right) = 0\,,\ \ \forall k \in K_r\,,\ \ r \in R\,,\ \ j = 1,\ldots,M \tag{3.12}$$
$$\pi_r^j - U_r^{k,j} \geq 0\,,\ \ \forall k \in K_r\,,\ \ r \in R\,,\ \ j = 1,\ldots,M \tag{3.13}$$
$$f_r^{k,j} \geq 0\,,\ \ \forall k \in K_r\,,\ \ r \in R\,,\ \ j = 1,\ldots,M\,, \tag{3.14}$$
$$\sum\nolimits_{k\in K_r} f_r^{k,j} - q_r^j = 0\,,\ \ \forall r \in R\,,\ \ j = 1,\ldots,M \tag{3.15}$$
$$v_a = \sum\nolimits_{j=1}^{M}\sum\nolimits_{r\in R}\sum\nolimits_{k\in K_r}\delta_{a,r}^k f_r^{k,j}\,,\ \ \forall a \in A \tag{3.16}$$
$$1 - \sum\nolimits_{k\in K_r}\lambda_r^{k,j} = 0\,,\ \ \forall r \in R\,, j = 1,\ldots,M \tag{3.17}$$
$$\varpi_r^j - \sum\nolimits_{k\in K_r}\lambda_r^{k,j}\zeta_r^k(\rho_r^j) = 0\,,\ \ \forall r \in R\,, j = 1,\ldots,M \tag{3.18}$$
$$\lambda_r^{k,j} \geq 0\,,\ \ \forall k \in K_r\,,\ \ r \in R\,,\ \ j = 1,\ldots,M \tag{3.19}$$
$$\zeta_r^k(\rho_r^j) - \varpi_r^j \geq 0\,,\ \ \forall k \in K_r\,,\ \ r \in R\,,\ \ j = 1,\ldots,M \tag{3.20}$$
$$g_r^j(x) = \begin{cases}(\varpi_r^j - x)^{\alpha}, x \leq \varpi_r^j \\ -\eta(x-\varpi_r^j)^{\beta}, x > \varpi_r^j\end{cases},\ \ \forall r \in R\,,\ \ j = 1,\ldots,M \tag{3.21}$$
$$U_r^{k,j} = \int_{\underline{t}_r^k}^{\varpi_r^j}\frac{dw((\psi_r^k(x))}{dx}g_r^j(x)dx + \int_{\varpi_r^j}^{\bar{t}_r^k} -\frac{dw(1-\psi_r^k(x))}{dx}g_r^j(x)dx\,,$$
$$\forall k \in K_r\,,\ \ r \in R\,,\ \ j = 1,\ldots,M \tag{3.22}$$

where q_r^j is the demand for traveler class *j* between O-D pair *r*. In the above, (3.12)-(3.16) define user equilibrium flow patterns; (3.17)-(3.20) determine reference points and (3.21) and (3.22) specify the calculation of the prospect value of each path.

The above conditions can be formulated as the following variational inequality:

$$G(X^*)\left(X - X^*\right) \geq 0\,,\ \ \text{For all } X \in \Lambda \tag{3.23}$$

With $X = \begin{pmatrix} f \\ \lambda \end{pmatrix}$, $G(X) = \begin{pmatrix} -U \\ \zeta \end{pmatrix}$ and

$$\Lambda = \left\{X \mid \sum\nolimits_k f_r^{k,j} = q_r^j, \forall r, j;\ 1 - \sum\nolimits_k \lambda_r^{k,j} = 0, \forall r, j;\ f_r^{k,j}, \lambda_r^{k,j} \geq 0, \forall r, k, j\right\}$$

where λ is a column vector of $\lambda_r^{k,j}$ whose dimension is $|K_r| \times |R| \times M$; U is a column vector of $U_r^{k,j}$ and ζ is a column vector of $\zeta_r^k(\rho_r^j)$ with the same dimension.

The equivalence between the variational inequality and the user equilibrium conditions (3.12)-(3.22) can be easily established by examining the optimality condition of the linear program $\min\limits_{X\in\Lambda} G(X^*)X$. Note that the above variational inequality does not involve π and ϖ. *U* in the above formulation is a function of *f* and λ, since π and ϖ are dual variables and at optimality $\varpi_r^j - \sum\nolimits_{k\in K_r}\lambda_r^{k,j}\zeta_r^k(\rho_r^j) = 0$. Therefore, the corresponding limits of the integrals in *U* can be replaced by $\sum\nolimits_{k\in K_r}\lambda_r^{k,j}\zeta_r^k(\rho_r^j)$. At the same time, ζ is parameterized by *f*, more specifically as $\zeta_r^k\left(f,\rho_r^j\right)$.

3.3.3 Model Property

As aforementioned, the marginal density function of the travel time, ψ_r^k, is parameterized by f. We further assume that the function is continuous with respect to f. Consequently, the inverse function ζ_r^k is continuous with f. With the value function and the probability function we introduced above, i.e., (3.21) and (3.3), it can be proved that $G(X)$ is continuous with X (see Appendix A for the proof). More specifically, $U_r^{k,j}$ is continuous with f and λ, and ζ_r^k is continuous with f. Given that Λ is compact and convex, there exists a solution to the above variational inequality (e.g., Harker and Pang, 1990).

We did not establish the uniqueness of the solution since $G(X)$ may not be strictly monotone on Λ due to the complicated function for the prospect values.

3.3.4 Connections with Models in the Literature

The proposed prospect-based user equilibrium model incorporates some user equilibrium models in the literature as special cases. Particularly with a single class of users,

- Let $\rho_r = 0$, $w(p) = p$, $\eta = 1$ and $\beta = 1$ in $g_r(x)$ defined in (3.5), then the prospect-based user equilibrium model reduces to the standard user equilibrium model in a stochastic network where travelers are assumed to make their route choice based on the average travel times;

- Let $\rho_r = 0$, $w(p) = p$, then the model reduces to the expected-utility-theory-based model proposed by Yin and Idea (2002);

- Let ϖ_r be fixed, then the model reduces to the CPT-based user equilibrium model formulated by Connors and Sumalee (2009);

- Let $w(p) = p$ and the reference point is with respect to each path, i.e., ω_r^k defined in (3.8), and $g_r^k(x) = -\omega_r^k$, then the model reduces to the travel time budget model developed by Lo et al. (2006).

- Let $w(p) = p$, $g_r(x) = \begin{cases} -x, & x \le \varpi_r \\ -x + \eta(\varpi_r - x), & x > \varpi_r \end{cases}$ and ϖ_r be fixed, then the model reduces to the late arrival penalty model proposed by Watling (2006).

- Let $w(p) = p$ and the reference point is with respect to each path, i.e., ω_r^k defined in (3.8), and $g_r^k(x) = \begin{cases} -\omega_r^k, & x \le \omega_r^k \\ -x, & x > \omega_r^k \end{cases}$, then the model reduces to the mean excess travel time model developed by Zhou and Chen (2008).

The above value functions reveal that the models by Watling (2006) and Zhou and Chen (2008) emphasize the late arrival penalty. Although both early and late arrivals are treated as penalty in the departure time choice models (e.g., Small, 1982), in route choice with given departure times, early arrival can be viewed as a gain because an earlier arrival implies less travel time than expected as well as other reduced costs associated with the time saved.

3.4 SOLUTION ALGORITHM AND NUMERICAL EXAMPLES

3.4.1 Solution Algorithm

The proposed variational inequality is a path-based formulation with non-additive cost structure (e.g., Lo and Chen, 2000). Although many existing algorithms to variational inequality may be applied to solve it, the complex form of the travel prospect makes them difficult to implement. In light of this, below we present a heuristic iterative algorithm to solve the variational inequality, with path enumeration. For large networks, another layer of column generation iteration should be added to avoid the cumbersome path enumeration (e.g., Lo and Chen, 2000; Yin and Ieda, 2001).

The algorithm is briefly described as follows:

Step 0: *Initialization*. Set $l = 1$ and specify an initial path flow pattern $f^{(l)}$ and the convergence tolerance ε.

Step 1: *Determination of reference points.* Based on the current flow pattern $f^{(l)}$, calculate the link flow pattern, and the path travel time distributions. Further determine the reference points that satisfy the constraints (3.17)-(3.20).

Step 2: *Calculation of prospect values.* Calculate the travel prospect value for each path according to (3.21) and (3.22).

Step 3: *Convergence check.* If $\left| f^{(l)T} \cdot G^{f^{(l)}}(X) \right| \le \varepsilon$, then stop. Otherwise, go to Step 4.

Step 4: *Path flows updating.* Find the search direction $g^{(l)}$ and step size $s^{(l)}$ based on the current flow and prospect value patterns, and update the path flow pattern as $f^{(l+1)} = f^{(l)} + s^{(l)} g^{(l)}$. Set $l = l+1$, go to step 1. For the search direction, let $g^{(l)} = \tilde{f}^{(l)} - f^{(l)}$. $\tilde{f}^{(l)}$ is an auxiliary flow pattern with $\tilde{f}_r^{k,j(l)} = q_r^j / m_r^j$ if $U_r^{k,j(l)} = \pi_r^{j(l)}$ and 0 otherwise, where m_r^j is the number of paths whose prospects are observed to be the maximal. The step size is set as follows: $s^{(l)} = \max\left(\frac{1}{100l}, 10^{-4}\right)$.

As described, the algorithm is essentially a method of successive average, which demonstrated a good convergence property in our numerical experiments. Other methods, such as the flow-swapping algorithm proposed by Huang and Lam (2002) and Yin et al. (2004) can also be applied to solve the problem. The algorithm is proved to be stable if the sequence of swapped flows is selected properly.

3.4.2 Numerical Examples

We first present a simple example to illustrate the proposed model. In this example, the proposed model is tailored to a specific case where the total O-D demand is assumed to be the source of uncertainty, following a normal distribution. More specifically, $Q_r \sim N(q_r, (cv \cdot q_r)^2)$ where Q_r is the stochastic O-D demand and *cv* denotes the coefficient of variance of the demand. It is further assumed that the path flows also follow normal distributions and have the same coefficient of variance with the O-D demands. The link travel time function is assumed to be the widely used BPR function, i.e., $t_a = t_a^0(1 + \beta_0 (v_a / C_a)^n)$, where t_a^0 is the free-flow travel time on link a and C_a is the link capacity. According to Shao et al. (2006), the distributions of path travel times can be derived as:

$$T_r^k \sim N(t_r^k, (\varepsilon_r^{k,t})^2), \quad \forall k \in K_r, \quad r \in R$$

where t_r^k and $(\varepsilon_r^{k,t})^2$ are the mean and variance of the path travel time, which can be further calculated via the following equations:

$$t_r^k = \sum_{a \in A} \delta_{a,r}^k \left(t_a^0 + t_a^0 \frac{\beta_0}{(c_a)^n} \sum_{i=1}^{n} \binom{n}{i} (\varepsilon_a^v)^i (v_a)^{n-i} (i-1)!! \right)$$

$$(\varepsilon_r^{k,t})^2 = \sum_{a \in A} \delta_{a,r}^k \left(t_a^0 \frac{\beta_0}{(c_a)^n} \right)^2 \cdot \left(\sum_{i=1}^{2n} \binom{2n}{i} (\varepsilon_a^v)^i (v_a)^{2n-i} (i-1)!! - \left(\sum_{i=1}^{n} \binom{n}{i} (\varepsilon_a^v)^i (v_a)^{n-i} (i-1)!! \right)^2 \right)$$

$$(\varepsilon_a^v)^2 = \sum_{r \in R} \sum_{k \in K_r} \delta_{a,r}^k (\varepsilon_r^{k,f})^2 = \sum_{r \in R} \sum_{k \in K_r} \delta_{a,r}^k (cv \cdot f_r^k)^2$$

where $(\varepsilon_a^v)^2$ and $(\varepsilon_r^{k,f})^2$ are the variances of the link and path flows respectively. As mentioned in Section 2.1, v_a and f_r^k denote the means of link and path flows. In essence, the above derivation determines how the path travel time distribution is parameterized by the average link flow pattern.

A toy network shown in Figure 3-3 is used in this example. There are four links between a single O-D pair (1-3).

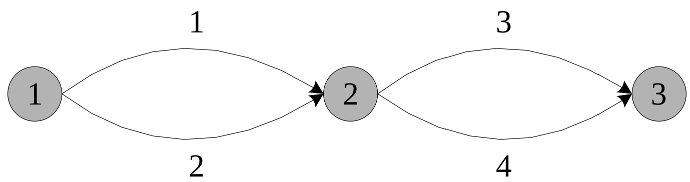

Figure 3-3. Four link network

The mean O-D demand and the coefficient of variance are assumed to be $q_r = 150$ and cv=0.1. The coefficients of the BPR function are $\beta_0 = 0.15$ and n=4. Link characteristics are as follows: t_1^0=15, t_2^0=20, t_3^0=15, t_4^0=10, C_1=90, C_2=90, C_3=100 and C_4=70.

The parameters of the value function in (3.5) are assumed to be α =0.37, β =0.59 and η =1.51, and the probability weighting function (3.3) is used with γ =0.74. We further assume that there are five classes of travelers whose demand portions and desired on-time arrival probabilities or OTAP, i.e., ρ_r^j in (3.10), are given in Table 3-1.

Table 3-1. Traveler Characteristics

Traveler Class	1	2	3	4	5
OATP (%)	40	50	60	70	80
Demand portion (%)	20	50	10	10	10

As previously stated in Section 3.2.1, in the case of stochastic O-D demand, the path flows are also stochastic. The path flow solutions generated from the prospect-based model are the mean values. The results of reference points (ϖ_r^j in Equation 3.10) and (average) path flows are presented in Table 3-2. As expected, class 1 of travelers with a lower desired on-time arrival probability will budget a less amount of travel time and thus possess a smaller reference point. Consequently, they prefer path 1, which offers a shorter mean travel time with a larger degree of variability. In contrast, classes 4 and 5 are more risk averse and thus have larger reference points. Path 3 is a safer choice for them. For class 2, paths 1 and 2 offer the same prospect values while paths 1 and 3 are indifferent for class 3. Those results are consistent with the CPT-based behavioral assumption and intuitively correct.

Table 3-2. Prospect-Based User Equilibrium Path Flow Pattern

Network topology						
Path number			1	2	3	4
Link Sequence			(1,3)	(1,4)	(2,3)	(2,4)
The proposed model						
Path travel time characteristics						
Average travel time			32.43	30.84	35.08	33.49
Standard deviation			5.31	9.07	0.12	7.36
Path choice behaviors of different classes						
Class	OTAP	Reference point	Path flow			
1	0.4	28.54	-	30.0	-	-
2	0.5	30.84	0.8	74.2	-	-
3	0.6	33.14	8.0	-	7.0	-
4	0.7	35.14	-	-	15.0	-
5	0.8	35.18	-	-	15.0	-
Total path flows			8.8	104.2	37.0	-

Table 3-3 compares the link flow solution to the proposed model with those from the prospect-based user equilibrium model with exogenous reference points and the standard user equilibrium model. For the former, two reference points, 25 and 30, are used, generating substantially different link flow patterns. It reconfirms that the determination of reference points is critical for applying the model. Note that the link flows with the reference point of 30 match closely with those from the proposed model. However, it is a formidable task to determine appropriate reference points beforehand, particularly when the flow pattern is unknown. Lastly, it can be observed that under the standard user equilibrium, the link flow pattern is significantly different than the one from the proposed model. The difference is certainly due to the different behavioral assumptions used in these models. The standard user equilibrium model does not consider travelers' risk-taking preferences. Therefore, if the travel time variability differs substantially among paths connecting the same O-D pair, the solution from the proposed model tends to differ from the standard user equilibrium flow pattern.

Table 3-3. Comparisons of Link Flow Patterns from Three Different UE Models

Link number	1	2	3	4
Prospect-based model with endogenous reference point	113.0	37.0	45.8	104.2
Prospect-based model with exogenous reference point ($\varpi_r = 25$)	140.6	9.4	34.1	115.9
Prospect-based model with exogenous reference point ($\varpi_r = 30$)	112.3	37.7	45.2	104.8
Standard user equilibrium model	140.2	9.9	35.1	115.0

The second numerical example below is to demonstrate the applicability of the proposed model and algorithm to larger networks and further explore the network characteristics under the prospect-based user equilibrium. A network with 13 nodes and 19 links from Nguyen and Dupuis (1984), as shown in Figure 3-4, is used in the numerical example.

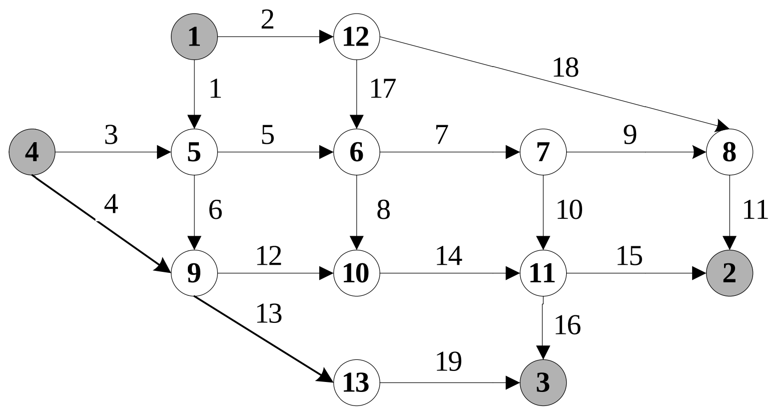

Figure 3-4. Nguyen and Dupuis's network

There are four O-D pairs in the network, 1-2, 1-3, 4-2 and 4-3 and the numbers of paths between those O-D pairs are 8, 6, 5 and 6, respectively. The O-D demands are deterministic and given as q_{1-2}=660, q_{1-3}=495, q_{4-2}=412.5, q_{4-3}=495. The average link travel time function is assumed to be the BPR function. Table 4 presents the link characteristics of the example network.

Considering day-to-day traffic incidents, travel times are assumed to be stochastic (e.g., Yin and Ieda, 2001; Yin et al., 2004). The marginal distribution of the travel time is assumed to be the following normal distribution:

$$T_r^k \sim N(t_r^k,\ \sigma_r^k \cdot t_r^k),\quad \forall k \in K_r,\quad r \in R \tag{3.24}$$

In the above, the mean is the average travel time of path *k,* determined through the BPR link travel time functions, and the variance is $\sigma_r^k \cdot t_r^k$, where σ_r^k is a variability parameter. In this numerical example, we first assume the variability parameters for those 25 paths in the network are $\sigma = \sigma_1$ = [0.5, 0.01, 0.15, 0.2, 0.1, 0.3, 0.001, 0.01; 0.3, 0.01, 0.3, 0.5, 0.02, 0.2, 0.1, 0.4, 0.001, 0.35, 0.02; 0.6, 0.1, 0.3, 0.05, 0.01, 0.1]$^{\mathrm{T}}$.

Table 3-4. Link Characteristics of the Example Network

Link	Free-Flow Travel Time	Capacity	Link	Free-Flow Travel Time	Capacity
1	7	300	11	9	500
2	9	200	12	10	550
3	9	200	13	9	200
4	12	200	14	6	400
5	3	350	15	9	300
6	9	400	16	8	300
7	5	500	17	7	200
8	13	250	18	14	300
9	5	250	19	11	200
10	9	300			

The parameters of the value function and the probability weighting functions are the same as in the above example. We further assume that each O-D pair has the same 11 classes of travelers whose desired on-time arrival probabilities or OTAP and demand portions are given in Table 3-5.

Table 3-5. Traveler Characteristics

Traveler Class	1	2	3	4	5	6	7	8	9	10	11
OATP (%)	40	45	50	55	60	65	70	75	85	95	99.9
Demand portion (%)	1.6	2.9	28.3	14.1	16.1	9.9	8.3	7.3	7	2.9	1.6

Solutions for two selected O-D pairs, 4-2 and 4-3, are presented below, and results for the other two O-D pairs are similar. As shown in Figure 3-5, travelers with different desired on-time arrival probabilities have different reference points and thus different prospect values for each path. Consequently, their route choices are different, as presented in Tables 3-6 and 3-7.

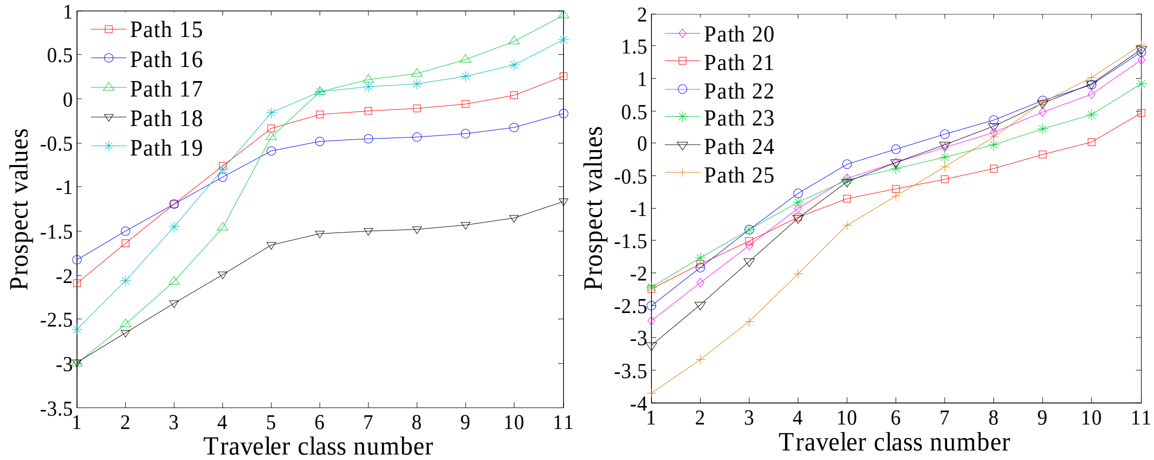

Figure 3-5. Prospect values of paths between O-D pairs 4-2 and 4-3

Table 3-6. Prospect-Based User Equilibrium Path Flow Pattern for O-D Pair 4-2 ($\sigma = \sigma_1$)

Path characteristics							
Path number (Link sequence)			15 (4,12, 14,15)	16 (3,5,7, 9,11)	17 (3,5,7, 10,15)	18 (3,5,8, 14,15)	19 (3,6,12, 14,15)
Mean travel time			89.50	88.63	90.35	91.33	89.91
Variability parameter			0.1	0.4	0.001	0.35	0.02
Time variance			8.95	35.45	0.09	31.96	1.80
Path choices							
Class	OTAP	Reference point	Path flow				
1	40%	87.12	-	6.60	-	-	-
2	45%	87.88	-	11.96	-	-	-
3	50%	88.63	59.48	57.26	-	-	-
4	55%	89.38	51.35	-	-	-	6.81
5	60%	90.14	-	-	-	-	66.41
6	65%	90.43	-	-	24.71	-	16.13
7	70%	90.51	-	-	34.24	-	-
8	75%	90.55	-	-	30.11	-	-
9	85%	90.66	-	-	28.87	-	-
10	95%	90.85	-	-	11.96	-	-
11	99.9%	91.28	-	-	6.60	-	-

As shown in Table 3-6, paths 15, 16, 17 and 19 of O-D pair 4-2 are utilized by different traveler classes in the user equilibrium. Among these four paths, path 16 has the shortest mean travel time but the largest variance while path 17 has the longest mean travel time but the smallest variance. Therefore, travelers with lower desired on-time probabilities and reference points, i.e., classes 1 and 2, choose path 16 over 17. In contrast, travelers with larger reference points, i.e., classes 7, 8, 9, 10 and 11, prefer path 17 to 16. For class 3, paths 15 and 16 offer the same prospect values. Similarly, paths 15 and 19 are both used by class 4 users while paths 17 and 19 are indifferent to class 6 users. Similar observations can be made from the path flow pattern between O-D pair 4-3 in Table 3-7. Particularly, path 20—the shortest path with largest variance—is not utilized by any user class. These observations are consistent with the ones from the first example. In general, if a trip is not important or the individual is risk-seeking, he or she tends to reserve less time and prefers a shorter path with greater uncertainty. On the other hand, for an important trip or a risk-averse traveler, a longer but more deterministic path is more preferable.

Table 3-7. Prospect-Based User Equilibrium Path Flow Pattern for O-D Pair 4-3 ($\sigma = \sigma_1$)

Path characteristics								
Path number (Link sequence)			20 (4,13,19)	21 (4,12, 14,16)	22 (3,6, 13,19)	23 (3,5,7, 10,16)	24 (3,5,8, 14,16)	25 (3,6,12, 14,16)
Mean travel time			108.69	109.74	109.11	110.60	111.58	110.16
Variability parameter			0.6	0.1	0.3	0.05	0.01	0.1
Time variance			65.22	10.97	32.73	5.53	1.12	11.02
Path choice								
Class	OTAP	Reference point	Path flow					
1	40%	106.65	-	-	7.91	-	-	-
2	45%	107.68	-	-	14.35	-	-	-
3	50%	108.69	-	34.89	105.19	-	-	
4	55%	109.71	-	69.79	-	-	-	-
5	60%	110.56	-	79.69	-	-	-	-
6	65%	111.02	-	49.00	-	-	-	-
7	70%	111.48	-	41.08	-	-	-	-
8	75%	111.98	-	36.13	-	-	-	-
9	85%	112.67	-	26.54	-	-	8.11	-
10	95%	113.32	-	-	-	-	14.35	-
11	99.9%	114.84	-	-	-	-	7.92	-

The travel time variability parameter partially represents the stochastic level of the network. A lower value of σ indicates that the network is less variable. To investigate the impact of σ on travelers' route choices, we set $\sigma = \sigma_2 = 0.5\sigma_1$. Again, we focus on O-D pairs 4-2 and 4-3. Figures 3-6 and 3-7 compare the equilibrium reference points and travel prospects of the 11 classes under different σ (σ_1 or σ_2). The results seem surprising. With a smaller value of σ, classes 1 and 2 between O-D pair 4-2 turn out to reserve more times, which leads to higher travel prospects, while classes 4 to 11 between O-D pair 4-2 reserve less time and the resulting travel prospects can be higher or lower (see Figure 3-6). The results are actually consistent with the trend when σ approaches zero. In that case, the reference point and prospect curves should become flat and the multiclass prospect-based user equilibrium reduces to a traditional single-class user equilibrium. Similar results are observed for O-D pair 4-3 (see Figure 3-7).

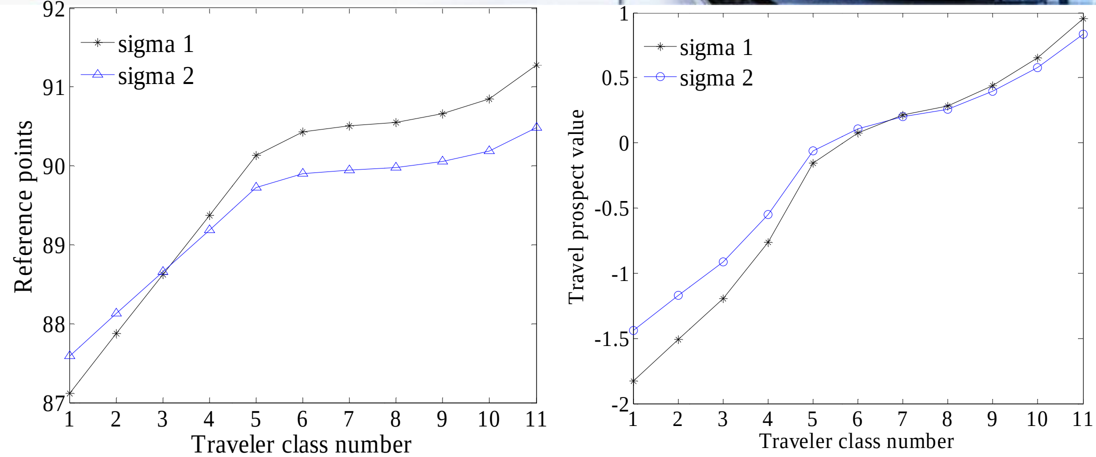

Figure 3-6. Equilibrium reference points and travel prospects between O-D pair 4-2

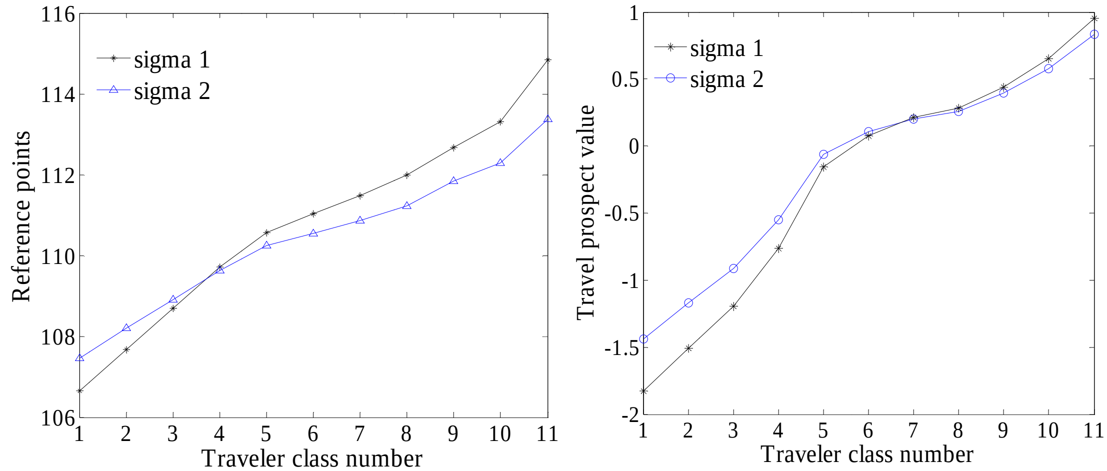

Figure 3-7. Equilibrium reference points and travel prospects between O-D pair 4-3

To scrutinize the impact of the level of stochasticity on travelers' route choices, we present the flow pattern between O-D pair 4-2 with $\sigma = \sigma_2$ in Table 3-8. Comparing Table 3-8 with 3-6, we observe that travelers of some classes change their route choices, particularly for those classes who utilized two paths originally. Taking class 3 for example, more travelers choose path 16 when σ decreases. The same is true for classes 4 and 6. For O-D pair 4-3, paths 20 and 23, which are not utilized before, become acceptable for some classes when the travel time variability is smaller.

Table 3-8. Prospect-based user equilibrium path flow pattern for O-D pair 4-2 ($\sigma = \sigma_2$)

Path characteristics							
Path number (Link sequence)			15 (4,12, 14,15)	16 (3,5,7, 9,11)	17 (3,5,7, 10,15)	18 (3,5,8, 14,15)	19 (3,6,12, 14,15)
Mean travel time			89.17	88.59	89.76	90.59	89.46
Variability Parameter			0.05	0.2	0.0005	0.175	0.01
Time variance			4.46	17.73	0.04	15.86	0.89
Path choice							
Class	OTAP	Reference point	Path flow				
1	40%	87.53	-	6.60	-	-	-
2	45%	88.06	-	11.96	-	-	-
3	50%	88.59	50.92	65.78	-	-	-
4	55%	89.12	56.26	-	-	-	1.86
5	60%	89.66	-	-	-	-	66.36
6	65%	89.83	-	-	15.04	-	25.77
7	70%	89.87	-	-	34.21	-	-
8	75%	89.90	-	-	30.11	-	-
9	85%	89.98	-	-	28.87	-	-
10	95%	90.11	-	-	11.96	-	-
11	99.9%	90.42	-	-	6.60	-	-

We now examine the system performance under the prospect-based user equilibrium. For this purpose, three measurers, i.e., total reserved time (TRT), total (mean) travel time (TTT) and total travel prospect (TTP), are defined as follows:

$$TRT = \sum_{r\in R} \sum_{j=1}^{M} \varpi_r^j q_r^j$$

$$TTT = \sum_{r\in R} \sum_{k\in K_r} \sum_{j=1}^{M} f_r^{k,j} t_r^k$$

$$TTP = \sum_{r\in R} \sum_{j=1}^{M} \pi_r^j q_r^j$$

The above three measures are computed in both scenarios, and the results are compared in Table 3-9. Some would expect a better system performance when the level of stochasticity decreases. Interestingly, as shown in Table 3-9, although the total reserved time decreases and the total travel prospect increases as expected, the total travel time increases. Apparently, travel times of some classes increase as the level of stochasticity decreases.

Table 3-9. Comparisons of System Performances

	TRT	TTP	TTT
$\sigma = \sigma_1$	1.9577e+005	-970.9208	1.9496e+005
$\sigma = \sigma_2 = 0.5\,\sigma_1$	1.9574e+005	-669.6350	1.9512e+005

3.5 BEHAVIORALLY CONSISTENT CONGESTION PRICING

To make pricing more efficient and effective, users' behavioral responses to pricing signals should be encapsulated into the pricing models. A number of behavioral studies have been undertaken to model how users respond to congestion pricing (e.g., Saleh and Farrell, 2005). However, the proposed modeling systems are often too complex to be incorporated in the pricing models. The gap between empirical behavioral models and the behavioral assumptions adopted in the pricing models is growing, and the challenge to bridging it is to seek a right balance between behavioral realism in and computational tractability of the pricing models.

The pricing model presented below represents one of the first attempts to develop more behaviorally consistent pricing models, where the prospect-based user equilibrium model presented above is applied to capture travelers' bounded rationality in response to the pricing signals.

3.5.1 Pricing Model Formulation

Travelers' route choice behaviors in the presence of tolls can be very complicated, and behavioral experiments are needed to gain a better understanding. However, this is beyond the scope of this chapter. In the following, we present two distinct behavioral conjectures and develop the pricing models to determine link-based tolls accordingly.

The first conjecture is that in the route choice travelers always view toll as a sure loss and consider the outcome as a gain only when the travel time they save can pay for the toll. With this conjecture, the reference points remain the same as in the no-toll case, and can be determined by (3.17)-(3.20). In other words, travelers still reserve a certain travel time based on travel time distributions, and this reserved time serves as the reference point in evaluating the outcome (generalized travel cost) of their route choice. The value function can thus be written as follows:

$$\hat{g}_r^{k,j}(x) = \begin{cases} (\varpi_r^j - \tau_r^k - x)^{\alpha}, x \le \varpi_r^j - \tau_r^k \\ -\eta(x + \tau_r^k - \varpi_r^j)^{\beta}, x > \varpi_r^j - \tau_r^k \end{cases} \tag{3.25}$$

where τ_r^k is the toll rate, in the unit of time, imposed on path k between O-D pair r, and is the sum of the tolls on the links that compose the path. Consequently, the prospect can be calculated as follows:

$$\hat{U}_r^{k,j} = \int_{\underline{t}_r^k}^{\varpi_r^j - \tau_r^k} \frac{dw((\psi_r^k(x))}{dx} \hat{g}_r^{k,j}(x)dx + \int_{\varpi_r^j - \tau_r^k}^{\bar{t}_r^k} -\frac{dw(1-\psi_r^k(x))}{dx} \hat{g}_r^{k,j}(x)dx \qquad (3.26)$$

Another plausible assumption is that travelers treat tolls essentially the same way as travel times. Through day-to-day learning, they identify the distribution of the generalized cost. The reference point is no longer the minimum ρ th percentile travel time for an O-D pair but rather the minimum ρ th percentile generalized travel cost. We denote a generalized travel cost as $\hat{T}_r^k = T_r^k + \tau_r^k$, and the marginal distribution function of the generalized travel cost as $\hat{\psi}_r^k$, which is in the same shape as ψ_r^k with a shift to the right by a distance of τ_r^k. With the above behavioral conjecture, the new reference points and the travel prospect values are written as follows:

$$1 - \sum_{k \in K_r} \lambda_r^{k,j} = 0, \quad \forall r \in R, j = 1, \ldots, M \qquad (3.27)$$

$$\hat{\varpi}_r^j - \sum_{k \in K_r} \lambda_r^{k,j} \left(\zeta_r^k(\rho_r^j) + \tau_r^k \right) = 0, \quad \forall r \in R, j = 1, \ldots, M \qquad (3.28)$$

$$\lambda_r^{k,j} \geq 0, \quad \forall k \in K_r, \quad r \in R, \quad j = 1, \ldots, M \qquad (3.29)$$

$$\zeta_r^k(\rho_r^j) + \tau_r^k - \hat{\varpi}_r^j \geq 0, \quad \forall r \in R, \quad j = 1, \ldots, M \qquad (3.30)$$

$$\hat{g}_r^j(x) = \begin{cases} (\hat{\varpi}_r^j - x)^\alpha, x \leq \hat{\varpi}_r^j \\ -\eta(x - \hat{\varpi}_r^j)^\beta, x > \hat{\varpi}_r^j \end{cases}, \quad \forall r \in R, \quad j = 1, \ldots, M \qquad (3.31)$$

$$\hat{U}_r^{k,j} = \int_{\underline{t}_r^k + \tau_r^k}^{\hat{\varpi}_r^j} \frac{dw((\hat{\psi}_r^k(x))}{dx} \hat{g}_r^j(x)dx + \int_{\hat{\varpi}_r^j}^{\bar{t}_r^k + \tau_r^k} -\frac{dw(1-\hat{\psi}_r^k(x))}{dx} \hat{g}_r^j(x)dx,$$
$$\forall k \in K_r, \quad r \in R, \quad j = 1, \ldots, M \qquad (3.32)$$

Note that both conjectures assume that travelers develop a good knowledge of the tolling structure during their day-to-day travels because the tolling structure is fixed and remains unchanged for a significant amount of time, say, one year.

To enhance the system performance, we seek a link toll pattern that either maximizes the total travel prospect or minimizes the total (expected) travel time. The optimal pricing model can be formulated as:

CP-1:

$$\max_{(\tau, f, \hat{\pi}, \hat{U}, \lambda, \varpi,)} \sum_{r \in R} \sum_{j=1}^{M} \hat{\pi}_r^j q_r^j \quad \text{or} \quad \min_{(\tau, f, \hat{\pi}, \hat{U}, \lambda, \varpi,)} \sum_{r \in R} \sum_{k \in K_r} \sum_{j=1}^{M} f_r^{k,j} t_r^k$$

s.t.

$$f_r^{k,j}\left(\hat{\pi}_r^j - \hat{U}_r^{k,j}\right) = 0 \qquad \forall k \in K_r, \quad r \in R, \quad j = 1, \ldots, M \qquad (3.33)$$

$$\hat{\pi}_r^j - \hat{U}_r^{k,j} \geq 0 \qquad \forall k \in K_r, \quad r \in R, \quad j = 1, \ldots, M \qquad (3.34)$$

(3.14)-(3.20)

(3.25)-(3.26)

$$\tau_r^k = \sum_a \delta_{a,r}^k \tau_a \qquad \forall k \in K_r, \quad r \in R \qquad (3.35)$$

$$\tau_a \geq 0 \qquad \forall a \in A \qquad (3.36)$$

CP-2:

$$\max_{(\tau, f, \hat{\pi}, \hat{U}, \lambda, \hat{\varpi})} \sum_{r\in R} \sum_{j=1}^{M} \hat{\pi}_r^j q_r^j \quad \text{or} \quad \min_{(\tau, f, \hat{\pi}, \hat{U}, \lambda, \hat{\varpi})} \sum_{r\in R} \sum_{k\in K_r} \sum_{j=1}^{M} f_r^{k,j} t_r^k$$

s.t. (3.14)-(3.16) and (3.27)-(3.36)

Both CP-1 and CP-2 are mathematical programs with complementarity constraints, a class of optimization problems difficult to solve because the problems are generally non-convex and violate the Mangasarian-Fromovitz constraint qualification at any feasible point (see, e.g., Scheel and Scholtes, 2000). Compounding the difficulty is the calculation of travel prospect values, which requires numerical integration.

3.5.2 Solution Algorithm

In view of that derivative-based methods may not be suitable to solve CP-1 or CP-2, this chapter adopts a simple derivative-free algorithm, the compass search, to solve the formulations for an illustration purpose. The compass search is among the earliest derivative-free algorithms developed (Kolda et al., 2003). The basic idea is to evaluate the objective function at an adjacent grid point defined by the coordinates and a certain grid size. If an adjacent grid point is a better solution, it then becomes the new iterate. If all the adjacent points are not better than the current solution, the grid size is reduced and the evaluation procedure will be repeated with the newly defined grid. The process continues until no better adjacent grid points can be found when the grid size is sufficiently small. Intuitively, the algorithm guarantees local optima. Many other derivative-free algorithms, such as the sequential simplex method (Nelder and Mead, 1965), are also applicable to CP-1 or CP-2. However, the compass search has been proved to be more reliable than others, although it is sometimes slow (Kolda et al., 2003).

Applying the compass search method to our pricing models, we evaluate a certain toll pattern by solving a tolled prospect-based user equilibrium model. Adjacent grid points are defined as toll patterns with only one link toll different from the current pattern by a predetermined grid size. The algorithm is described as follows:

Step 0: *Initialization*. Let *D* be the set of coordinate directions. $D = \{\pm e_i \mid i = 1,2,...|A|\}$, where e_i is the i^{th} unit coordinate vector in $R^{|A|}$. Select an initial link toll pattern τ^0, an initial grid size parameter Δ^0, and a convergence criterion ε. Set $l = 0$.

Step 1: *Evaluation of adjacent grid points.* If there is some $d_k \in D$ such that the new toll pattern $\tau^l + \Delta^l d_k$ is feasible and leads to a better objective function value (system performance), then set $\tau^{l+1} = \tau^l + \Delta^l d_k$, $\Delta^{l+1} = \Delta^l$, $l = l + 1$, and repeat step 1.

Step 2: *Convergence check.* If every $\tau^l + \Delta^l d_k$ is inferior to τ^l (including infeasible toll pattern), then compare Δ^l with ε. If $\Delta^l > \varepsilon$, set $\Delta^{l+1} = \frac{1}{2}\Delta^l$, $\tau^{l+1} = \tau^l$, $l = l + 1$, and go to step 1. Otherwise, stop.

3.5.3 Numerical Example

CP-1 with the objective function of minimizing the total (expected) travel time is solved for Nguyen and Dupuis's network as shown in Figure 4 and Table 3. For simplicity, we consider one single class of travelers with a desired on-time arrival probability of 90 percent. The variability parameter in the path travel time distribution is set to be σ_1. The parameters of the value function in (3.25) are assumed to be $\alpha = \beta = 0.52$ and $\eta = 2.25$ and another widely used probability weighting function derived by Prelec (1998), i.e., $w(p) = \exp\left(-\left[-\ln(p)\right]^\gamma\right)$, is used in this example with γ being 0.74.

Table 3-10 presents the resulting optimal toll pattern (in the unit of time) and the corresponding tolled user equilibrium flow pattern. The total expected travel time is reduced from 201527.3 to 193831.4, a 3.82 percent reduction. Comparing with the system optimum where the total (expected) travel time is 193823.5, the pricing scheme achieves 99.90 percent of the possible reduction for this particular network. Figure 3-8 is a convergence plot of the compass search algorithm. The algorithm finds a good solution quickly but spends a lot of resource in verifying the final solution.

Table 3-10. Optimum Toll Pattern and the Tolled Prospect-Based User Equilibrium Flow

Link	Toll Rate	Link Flow	Link	Toll Rate	Link Flow
1	0.00	700.85	11	1.00	706.46
2	1.00	454.15	12	0.00	580.81
3	0.00	464.08	13	4.00	360.76
4	5.02	443.42	14	0.00	617.18
5	5.00	666.77	15	0.00	366.04
6	0.00	498.16	16	0.00	629.24
7	1.00	701.03	17	0.00	70.62
8	0.00	36.37	18	1.00	383.53
9	0.00	322.93	19	1.00	360.76
10	1.00	378.09			

Table 3-11 further displays the detailed path flow pattern for O-D pair 1-3 and the corresponding path travel time, toll rate, and prospect value. The results illustrate that the prospect-based user equilibrium conditions are satisfied. Path 13 is not utilized largely due to its poor reliability although it is toll free. Path 9 is not utilized either although it is among the most reliable paths. With a relatively long travel time, a small standard deviation and a non-ignorable toll rate, a traveler would rarely experience a gain from using this path. On the other hand, path 10 with the longest travel time is utilized largely due to a low toll rate and a reasonable standard deviation. Similar results can be observed for other O-D pairs, which demonstrate that travelers are seeking a three-way balance among the expected travel time, variability of travel time and toll.

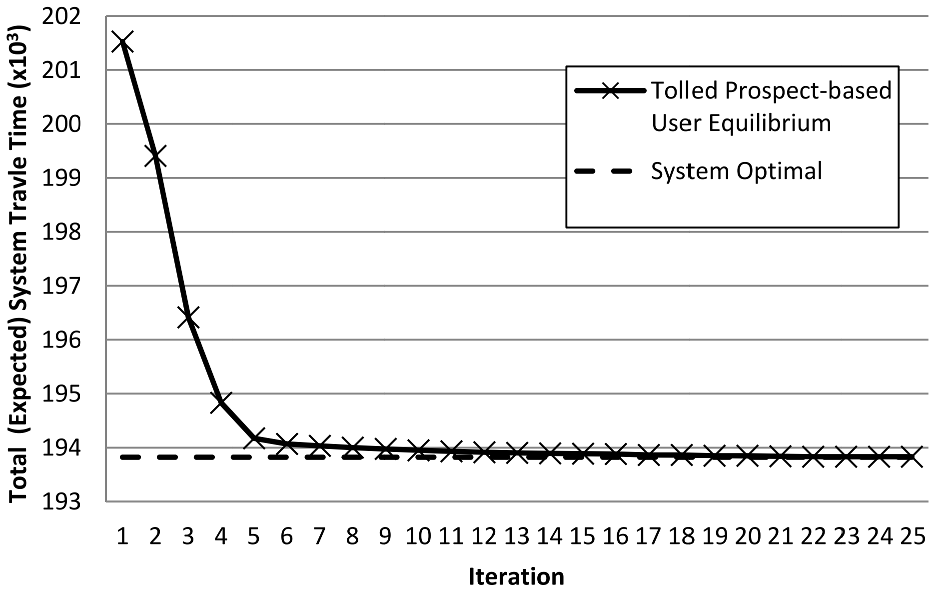

Figure 3-8. Convergence plot

Table 3-11 Tolled Prospect-Based User Equilibrium Path Flow Pattern for O-D Pair 1-3 ($\sigma = \sigma_1$)

Path Number (Link Sequence)	9 (2,7,10, 16,17)	10 (2,8,14, 16,17)	11 (1,5,7 9,16)	12 (1,5,8, 14,16)	13 (1,6,12, 14,16)	14 (1,6, 13,19)
Mean Travel Time	103.44	107.24	98.73	102.53	104.71	102.28
Travel Time Standard Deviation	2.13	21.65	1.06	32.23	52.36	32.18
Path Toll Rate	3.00	1.00	6.00	5.00	0.00	5.00
Prospect	-5.79	-5.56	-5.56	-5.63	-5.82	-5.56
Path Flow	0.00	35.09	99.15	0.00	0.00	360.76

Appendix A: Continuity proof of *G*(*X*)

$$
\begin{aligned}
&\left|G(X+\Delta X)-G(X)\right| \\
&=\left|\begin{pmatrix}-U(f+\Delta f,\lambda+\Delta\lambda)\\ \zeta(f+\Delta f)\end{pmatrix}-\begin{pmatrix}-U(f,\lambda)\\ \zeta(f)\end{pmatrix}\right| \qquad \text{(A1)}\\
&\le\left|\begin{pmatrix}-U(f+\Delta f,\lambda+\Delta\lambda)\\ \zeta(f+\Delta f)\end{pmatrix}-\begin{pmatrix}-U(f,\lambda+\Delta\lambda)\\ \zeta(f)\end{pmatrix}\right|+\left|\begin{pmatrix}-U(f,\lambda+\Delta\lambda)\\ \zeta(f)\end{pmatrix}-\begin{pmatrix}-U(f,\lambda)\\ \zeta(f)\end{pmatrix}\right|
\end{aligned}
$$

It is assumed that ψ is continuous with respect to *f*, then ζ is continuous with respect to *f*, i.e. $\lim_{\Delta f\to 0}|\zeta(f+\Delta f)-\zeta(f)|=0$.

Consider the first two items in (A1). Let $z_r^j(f,\lambda)=\sum_k \lambda_r^{k,j}\zeta_r^k(f,\rho_r^j)$, we have

$$
\begin{aligned}
&\left|U(f+\Delta f,\lambda+\Delta\lambda)-U(f,\lambda+\Delta\lambda)\right| \\
&=\Bigg|\int_{\underline{t}}^{z(f+\Delta f,\lambda+\Delta\lambda)}\frac{dw(\psi(f+\Delta f,x))}{dx}g(f+\Delta f,\lambda+\Delta\lambda,x)dx-\int_{\underline{t}}^{z(f,\lambda+\Delta\lambda)}\frac{dw(\psi(f,x))}{dx}g(f,\lambda+\Delta\lambda,x)dx \\
&+\int_{z(f+\Delta f,\lambda+\Delta\lambda)}^{\bar{t}}\frac{-dw(1-\psi(f+\Delta f,x))}{dx}g(f+\Delta f,\lambda+\Delta\lambda,x)dx-\int_{z(f,\lambda+\Delta\lambda)}^{\bar{t}}\frac{-dw(1-\psi(f,x))}{dx}g(f,\lambda+\Delta\lambda,x)dx\Bigg| \\
&\le\left|\int_{\underline{t}}^{z(f,\lambda+\Delta\lambda)}\left[\frac{dw(\psi(f+\Delta f,x))}{dx}g(f+\Delta f,\lambda+\Delta\lambda,x)-\frac{dw(\psi(f,x))}{dx}g(f,\lambda+\Delta\lambda,x)\right]dx\right| \\
&+\left|\int_{z(f,\lambda+\Delta\lambda)}^{z(f+\Delta f,\lambda+\Delta\lambda)}\frac{dw(\psi(f+\Delta f,x))}{dx}g(f+\Delta f,\lambda+\Delta\lambda,x)dx\right| \\
&+\left|\int_{z(f+\Delta f,\lambda+\Delta\lambda)}^{\bar{t}}\left[\frac{-dw(1-\psi(f+\Delta f,x))}{dx}g(f+\Delta f,\lambda+\Delta\lambda,x)-\frac{-dw(1-\psi(f,x))}{dx}g(f,\lambda+\Delta\lambda,x)\right]dx\right| \\
&+\left|\int_{z(f,\lambda+\Delta\lambda)}^{z(f+\Delta f,\lambda+\Delta\lambda)}\frac{-dw(1-\psi(f,x))}{dx}g(f,\lambda+\Delta\lambda,x)dx\right|
\end{aligned}
$$

In the above, the right-hand side approaches zero when Δf is arbitrarily small. Therefore, $\lim_{\Delta f\to 0}\left|U(f+\Delta f,\lambda+\Delta\lambda)-U(f,\lambda+\Delta\lambda)\right|=0$. For the last two items in (A1), it can be proved similarly that $\lim_{\Delta\lambda\to 0}\left|U(f,\lambda)-U(f,\lambda+\Delta\lambda)\right|=0$. Therefore, *U* is continuous with respect to *f* and λ.

This completes the proof that $\lim_{\Delta X\to 0}\left|G(X+\Delta X)-G(X)\right|=0$.

4 CONCLUDING REMARKS

The report presents methodologies to proactively account for travelers' boundedly rational route choice behaviors in urban transportation networks and determine pricing strategies that are based on more realistic behavioral assumptions and can relieve congestion more effectively. The investigation considers both deterministic and stochastic networks.

For deterministic networks, this report provides mathematical definitions of BRUE based on path and link flows. The set of BRUE flow distributions is non-empty and generally non-convex. Robust pricing models are formulated to minimize the maximum system travel time realized from the set of tolled BRUE flow distributions. Numerical experiments demonstrate that system performance may vary substantially within the set of BRUE flow distributions and the proposed robust pricing models are able to guard against the worst-case scenario effectively.

For stochastic networks, this report uses the cumulative prospect theory to model travelers' route choice behaviors under risk and develops a prospect-based user equilibrium model. This model incorporates the determination of reference points based on a premise that the point for an individual is the time he or she budgeted to ensure his or her desired on-time arrival probability. The model is flexible and general. By changing the specification of the value and weighting functions and the determination of reference points, the proposed prospect-based model reduces to a variety of user equilibrium models proposed in the literature. Applying the proposed prospect-based user equilibrium model to capture travelers' response to pricing signals, this report also develops a pricing model to maximize the total travel prospects or minimize the total (expected) travel times. To describe travelers' route choice behaviors under uncertainty and in the presence of tolls, two hypotheses are proposed. The pricing scheme for this model is based on more realistic behavioral assumptions and thus more likely to achieve the expected outcome.

Traffic congestion is one of the most severe problems that threaten the economic prosperity and quality of life in many societies. According to a report from Texas Transportation Institute, it caused approximately a loss of $87.2 billion in 2007 in the urban areas of United States. The results from this report will help reducing traffic congestion by changing travel behaviors via charging the correct amount of toll at the right place and time.

REFERENCE

Ahuja, R., Magnanti, T., Orlin, J. (1993) *Network Flows: Theory, Algorithms, and Applications*. The Prentice-Hall Inc., Upper Saddle River, New Jersey.

Avineri, E. (2004) A cumulative prospect theory approach to passengers' behavior modeling: waiting time paradox revisited. *Journal of Intelligent Transportation Systems,* 8(4), 195-204.

Avineri, E. (2006) The effect of reference point on stochastic network equilibrium. *Transportation Science,* 40(4), 409-420.

Avineri, E., Prashker, J.N. (2003) Sensitivity to uncertainty: the need for a paradigm shift. *Transportation Research Record*, 1854, 90-98.

Avineri, E., Prashker, J.N. (2004) Violations of expected utility theory in route-choice stated preferences: the certainty effect and inflating of small probabilities. *Transportation Research Record,* 1894, 222-229.

Bazaraa, M.S., Sherali, H.D., Shetty, C.M. (2006) *Nonlinear Programming: Theory and Algorithms*. John Wiley & Sons, Inc., Hoboken, New Jersey.

Beckmann, M.J., McGuire, C.B., Winsten, C.B. (1956) *Studies in Economics of Transportation*. Yale University Press, New Haven, Conn.

Ben-Tal, A., Nemirovski, A. (2002) Robust optimization — methodology and applications. *Mathematical Programming Series B,* 92(3), 453 – 480.

Bertsimas, D., Tsitsiklis, J.N. (1997) *Introduction to Linear Optimization*. Athena Scientific, Nashua, NH.

Bogers, E.A.I., Zuylen, H.J. (2004) The importance of reliability in route choices in freight transport for various actors on various levels. *Proceedings of European Transport Conference*. Strasbourg, France.

Bonsall, P., Shires, J., Maule, J. Matthews, B., Beale, J. (2007) Response to complex signals: theory, evidence and implications for road pricing. *Transportation Research, Part A*, 41(7), 672-683.

Brooke, A., Kendrick, D., Meeraus, A., Raman, R. (2003) *GAMS: A User's Guide*, GAMS Development Corporation, Washington, DC.

Camerer, C. F., Ho, T.-H. (1994) Violations of the betweenness axiom and nonlinearity in probability. *Journal of Risk and Uncertainty*, 8(2), 167-196.

Chen, H.-C., Friedman, J.W., Thisse, J.-F. (1997) Boundedly rational Nash equilibrium: a probabilistic choice approach. *Games and Economic Behavior*, 18(1), 32-54

Chen, R. B., Mahmassani, H.S. (2009). Learning and risk attitudes in route choice dynamics. *The Expanding Sphere of Travel Behaviour Research: The Proceedings of 11th International Conference* (edited by Kitamura, R. and Yoshii, T.), 791-818.

Conlisk, J. (1996) Why bounded rationality. *Journal of Economic Literature*, 34, 669-700.

Connors, R.D., Sumalee, A. (2009) A Network equilibrium model with travelers' perception of stochastic travel times. *Transportation Research Part B*, 43(6), 614-624.

Daganzo, C.F., Sheffi, Y. (1977) On stochastic models of traffic assignment. *Transportation Science*, 11(3), 253-274.

Drud, A.S. (1995) A system for largescale nonlinear optimization. *Tutorial for CONOPT Subroutine Library*, ARKI Consulting and Development A/S, Bagsvaerd, Denmark.

Florian, M., Hearn, D. (1990) Chapter 11 network equilibrium and pricing, *Handbook of Transportation Science* (edited by Hall, R.), Kluwer Academic Publishers.

Fujii, S., Kitamura, R. (2004) Drivers' mental representation of travel time and departure time choice in uncertain traffic network conditions. *Networks and Spatial Economics,* 4(3), 243-256.

Harker, P.T., Pang, J.S. (1990) Finite-dimensional variational inequality and nonlinear complementarity problems: a survey of theory, algorithms and applications. *Mathematical Programming*, 48(2), 161-220.

Hearn, D.W., Ramana, M.V. (1998) Solving congestion toll pricing models, *Equilibrium and Advanced Transportation Modeling* (edited by Marcotte, P. and Nguyen, S.), Kluwer Academic Publishers, Nowell, MA, 109-124.

Holguin-Veras, J., Xu, N., Wang, Q., Ozbay, K., Zorrilla, J.C. and Cetin, M. (2007) New Jersey Turnpike time-of-day pricing initiative's behavioral impacts. *Transportation Research Record*, 2010, 53-61.

Hu, T.-Y., Mahmassani, H.S. (1997) Day-to-day evolution of network flows under real-time information and reactive signal control. *Transportation Research Part C*, 5(1), 51-69.

Huang, H., Lam, W.H.K. (2002) Modeling and solving the dynamic user equilibrium route and departure time choice problem in network with queues. *Transportation Research Part B*, 36(3), 253-273.

Jayakrishnan, R., Mahmassani, H.S., Hu, T.-Y. (1994) An evaluation tool for advanced traffic information and management systems in urban networks. *Transportation Research Part C*, 2(3), 129-147.

Jou, R.C., Kitamura, R., Weng, M.C., Chen, C.C. (2008) Dynamic commuter departure time choice under uncertainty. *Transportation Research Part A,* 42(5), 774-783.

Kahneman, D., Tversky, A. 1979. Prospect theory: An analysis of decisions under risk. *Econometrica*, 47(2), 263–291.

Katsikopoulos, K.V., Fisher, D.L., Duse-Anthony, Y., Duffy, S.A. (2002) Risk attitude reversals in drivers' route choice when range of travel time is provided. *Human Factors,* 44(3), 466-473.

Knight, F.H. (1924) Some fallacies in the interpretation of social costs. *Quarterly Journal of Economics*, 38(4), 582-606.

Kolda, T., Lewis, R., Torczon, V. (2003) Optimization by direct search: new perspectives on some classical and modern methods. *SIAM Review*, 45(3), 385-482

Koszegi, B., Rabin, M. (2006) A model of reference-dependent preferences. *Quarterly Journal of Economics*, 121(4), 1133-1165.

Lam, W.H.K., Shao, H., Sumalee, A. (2008) Modeling impacts of adverse weather conditions on a road network with uncertainties in demand and supply. *Transportation Research Part B,* 42(10), 890-910.

Lawphongpanich, S., Yin, Y. (2010) Solving Pareto-improving congestion pricing for general road networks, *Transportation Research Part C*, 18, 234-246.

LeBlanc, L.J., Morlok, E.K., and Pierskalla, W.P. (1975) An efficient approach to solving the road network equilibrium traffic assignment problem. *Transportation Research*, 9(5), 309-318.

Lindsey, R. (2006) Do economists reach a conclusion on road pricing? The intellectual history of an idea. *Econ Journal Watch*, 3(2), 292-379.

Lo, H.K., Chen, A. (2000) Traffic equilibrium problem with route-specific costs: formulation and algorithms. *Transportation Research Part B*, 34(6), 493-513.

Lo, H.K., Luo, X.W., Siu, B.W.Y. (2006) Degradable transport network: travel time budget of travelers with heterogeneous risk aversion. *Transportation Research Part B,* 40(9), 792-806.

Lou, Y., Yin, Y., Lawphongpanich, S. (2010) Robust congestion pricing under boundedly rational user equilibrium. *Transportation Research Part B*, 44(1), 15-28.

Lopez, M., Still, G. (2007) Semi-infinite programming. *European Journal of Operations Research*, 119(2), 301-313.

Luo, Z.-Q., Pang, J.-S., Ralph, D. (1996) *Mathematical Programs with Equilibrium Constraints*, Cambridge University Press, New York, New York.

Mahmassani, H.S. (2000) Trip timing, *Handbook of Transport Modeling* (edited by Hensher, D.A. and Button, K.J.), Elsevier, New York, New York, 393-405.

Mahmassani, H.S., Chang, G.L. (1987) On boundedly-rational user equilibrium in transportation systems. *Transportation Science*, 21(2), 89-99.

Mahmassani, H.S., Liu, Y.-H. (1999) Dynamic of commuter decision behavior under advanced traveler information. *Transportation Research Part C*, 7(2-3), 91-108.

Mirchandani, P., Soroush, H. (1987) Generalized traffic equilibrium with probabilistic travel-times and perceptions. *Transportation Science*, 21(3), 133-152.

Munro, A., Sugden, R. (2003) On the theory of reference-dependent preferences. *Journal of Economic Behavior & Organization,* 50(4), 407-428.

Nakayama, S., Kitamura, R., Fujii, S. (2001) Drivers' route choice rules and network behavior: do drivers become rational and homogeneous through learning*? Transportation Research Record*, 1752, 62-68.

Neilson, W., Stowe, J. (2002) A further examination of cumulative prospect theory parameterizations. *Journal of Risk and Uncertainty,* 24(1), 31-46.

Nguyen, S., Dupuis, C. (1984) An efficient of method for computing traffic equilibria in networks with asymmetric transportation costs. *Transportation Science,* 18(2), 185-202.

Patriksson, M. (1994) *The Traffic Assignment Problem: Models and Methods*, VSP, Utrecht, Netherlands.

Pesendorfer, W. (2006) Behavioral economics comes of age. *Journal of Economic Literature*, 44(3), 712-721.

Pigou, A.C. (1920) *The Economics of Welfare*, MacMillan, New York, NY.

Polak, E., Royset, J. (2005) On the use of augmented Lagrangians in the solution of generalized semi-infinite min-max problems. *Computational Optimization and Applications*, 31(2), 173 – 192.

Prelec, D. (1998) The probability weighting function. *Econometrica*, 66(3), 497-527.

Saleh, W., Farrell, S. (2005) Implications of congestion charging for departure time choice: work and non-work schedule flexibility. *Transportation Research Part A*, 39(7-9), 773-791.

Scheel, H., Scholtes, S. (2000) Mathematical programs with complementarity constraints: stationarity, optimality, and sensitivity. *Mathematics of Operations Research*, 25(1), 1-22.

Schmidt, U., Starmer, C., Sugden, R. (2008) Third-generation prospect theory. *Journal of Risk and Uncertainty*, 36(3), 203-223.

Schmidt, U., Zank, H. (2010) Endogenizing prospect theory's reference point. Kiel Working Paper No. 1611, available at *http://www.ifw-members.ifw-kiel.de/publications/endogenizing-prospect-theory-s-reference-point/kwp_1611,* May 5th, 2010.

Schwanen, T., Ettema, D. (2009) Coping with unreliable transportation when collecting children: Examining parents' behavior with cumulative prospect theory. *Transportation Research Part A*, 43(5), 511-525.

Shao, H., Lam, W.H.K., Tam, M.L. (2006) A reliability-based stochastic assignment model for network with multiple user classes under uncertainty in demand. *Network and Spatial Economics,* 6(3-4), 173-204.

Sheffi, Y. (1985) *Urban Transportation Networks: Equilibrium Analysis with Mathematical Programming Methods*, Prentice-Hall Inc.

Small, K. A. (1982) The scheduling of consumer activities: work trips. *American Economic Review*, 72(3), 467-479.

Still, G. (1999) Generalized semi-infinite programming: theory and methods. *European Journal of Operations Research*, 119(2), 301 – 313.

Sumalee, A., Connors, R.D., Luathep, P. (2009) Network equilibrium under cumulative prospect theory and endogenous stochastic demand and supply. *Transportation and Traffic Theory 2009: Golden Jubilee*, 19-38.

Szeto, W.Y. and Lo, H.K., 2006. Dynamic traffic assignment: properties and extensions. *Transportmetrica*, 2(1), 31-52.

Thaler, R. H., Tversky, A., Kahneman, D., Schwartz, A. (1997) The effect of myopia and loss aversion on risk taking: An experimental test. *Quarterly Journal of Economics*, 112(2), 647-661.

Tversky, A., Kahneman, D. (1992) Advances in prospect theory: cumulative representation of uncertainty. *Journal of Risk and Uncertainty,* 5(4): 297-323.

U.S. Department of Transportation (2006) *National Strategy to Reduce Congestion on America's Transportation Network*.

Viti, F., Bogers, E., Hoogendoorn, S. (2005) Day-to-day learning under uncertainty with information provision: model and data analysis. *Paper Presented at the 16th International Symposium of Transportation and Traffic Theory,* College Park, MD.

Wardrop, J.G. (1952) Some theoretical aspects of road traffic research. *Proceeding of Institute of Civil Engineers*, Part II, 325-378.

Watling, D. (2006) User equilibrium traffic network assignment with stochastic travel times and late arrival penalty. *European Journal of Operational Research,* 175(3), 1539-1556.

Wie, B.W. (2007) Dynamic Stackelberg equilibrium congestion pricing. *Transportation Research Part C*, 15, 154-174.

Yang, H., Huang, H.-J. (2005) *Mathematical and Economic Theory of Road Pricing*, Elsevier.

Yin, Y., Ieda, H. (2001) Assessing performance reliability of road networks under non-recurrent congestion. *Transportation Research Record*, 1771, 148-155

Yin, Y., Lam, W.H.K., Ieda, H. (2004) New technology and the modeling of risk-taking behavior in congested road networks. *Transportation Research Part C*, 12(3-4), 171-192.

Yin, Y., Lawphongpanich, S. (2007) A robust approach to the continuous network design problem with demand uncertainty. *Transportation and Traffic Theory 2007: Papers Selected for Presentation at ISTTT17, A Peer Reviewed Series Since 1959* (edited by Allsop, R.E., Bell, M.G.H., Heydecker, B.G.), Elsevier, 111-126.

Zhou, Z., Chen, A. (2008) Comparative analysis of three user equilibrium models under stochastic demand. *Journal of Advanced Transportation,* 42(3), 239-263.

Zhou, J., Xu, H., Xu, W. (2009) A decision-making rule in traveler's route choice behavior based on cumulative prospect theory. *Poster Presented at the 18th International Symposium of Transportation and Traffic Theory*, Kowloon, Hong Kong.